Structural and geochronological analysis of the Walter-Outalpa retrograde shear zone in the eastern Weekeroo inlier. Olary Domain, South Australia.

Anthony Nicholas Bottrill B. Sc.

Department of Geology and Geophysics
The University of Adelaide

1998

This thesis is submitted as a partial fulfilment for the
Honours Degree of Bachelor of Science

Australian National Grid Reference

(SI 54 - 2) 1:250, 000

ABSTRACT

The Walter-Outalpa shear zone is NW trending, and forms a conjugate structure to the more numerous and documented E-ENE and NE trending shear zones of the Olary Domain. The Walter-Outalpa shear zone is 10km long, and bounded to the west by a western margin thrust zone, and to the east by an unconformable contact with the Adelaidean Supergroup.

The geometry of the Walter-Outalpa shear zone is confined to its Delamerian reactivation because of marked overprinting. During the Delamerian, the shear zone was reactivated as a southerly dipping dextral oblique system, with some reverse movement. The shear zone displays both ductile and brittle structures from this reactivation. Compression was approximately N-S, and retrogression of mineral assemblages to greenschist facies occurred.

Structures in the shear zone indicate dextral movement both pre-Adelaidean, and during Delamerian reactivation. Horizontal offset of the Willyama Supergroup units (eg. the Walter-Outalpa Granite) is up to 3,500m. This is much greater than offsets previously reported for the Olary Domain, and much greater than the offset seen at the basement-cover unconformity (between the Willyama and Adelaidean Supergroups). This indicates a long pre-Adelaidean history for the Walter-Outalpa shear zone. The basal conglomerate of the Adelaidean Supergroup however, does show evidence of shearing, and structures and fabrics within the shear zone also indicate reactivation during the Delamerian.

The Walter-Outalpa retrograde shear zone, within the eastern Weekeroo inlier, truncates all Willyama Supergroup lithologies and structures. It does not, however, truncate Adelaidean Supergroup lithologies and is therefore interpreted as a post-Olarian Orogeny, but pre-Adelaidean structure. However, reactivation of the Walter-Outalpa shear zone occurred during the Delamerian deformation. Many fabrics and structures within the shear zone represent this Delamerian overprint, as indicated by Sm-Nd dating of a garnet-chlorite schist which only occurs within the shear zone. A four point isochron, including garnet, chlorite, muscovite, and biotite, gives an age of 509 ± 19 Ma.

ENE trending shear zones show U and REE mineralisation (eg. Radium Hill, Crockers Well), and some shear zones act as structural traps for mineralisation (eg. White Dam deposit). No previous work has studied the geometry, kinematics, and interactions of retrograde shear zones within the Olary Domain. Understanding of the features related to retrograde shear zones may provide valuable information for major Olary Domain mineralisation exploration. The Walter-Outalpa shear zone provides a useful example for analogy with other shear zone studies within the Olary Domain.

TABLE OF CONTENTS

List of Figures

List of Plates

Plate 1

1.a Minor-scale shear band which displays localisation of shear strain, typical of shear zones. Broken up quartz veins within the shear band show that there is also localisation of hydrothermal fluids.

1.b Minor-scale riedel shear planes transecting and offsetting the more competent quartzofeldspathic layers. Mica-rich interlayers preserve more ductile deformation. Indicates dextral shearing.

1.c Minor-scale anti-riedel shear planes transecting and offsetting a pegmatitic intrusion into the Layered Gneiss unit. Indicates dextral shearing.

1.d Typical appearance of the Migmatitic Gneiss unit on a freshly exposed surface.

1.e Layer parallel (S_1) fabric within the IPMS unit. The black pen defines the strike of the S_1 fabric. The yellow pencil defines the strike of a weak S_2 fabric.

1.f Remnant original layering preserved within calc-silicate.

1.g Typical appearance of the Layered Gneiss unit on a freshly exposed surface.

Plate 2

2.a Minor-scale brittle shearing in the Southern Quartzofeldspathic Gneiss unit. Unit is sheared dextrally.

2.b Protomylonitic ductile 'fins' of shearing which form 2m high outcrops of the Retrograde Schist unit. Outcrop displays dextral shearing.

2.c Minor-scale F_2 fold within the IPMS unit. Strong axial planar (S_2) fabric which is at a low angle to the layer parallel S_1 fabric. Within the fold hinge, the S_1 fabric is overprinted.

2.d Minor-scale F_3 fold within the Layered Gneiss unit.

2.e Minor-scale S-C fabrics within a protomylonitic shear band. Represent dextral shearing.

2.f Minor-scale S-C fabric orientations are influenced locally, especially by the presence of more competent structures. Asymmetry of pegmatitic boudin indicates dextral shearing.

2.g Minor-scale riedel and anti-riedel shear planes present in the same outcrop, and also the same layer of the Layered Gneiss unit. Consistent with dextral shearing.

2.h Minor-scale 'pop up' structure formed within the IPMS unit close to the shear zone.

Plate 3

3.a Minor-scale asymmetric shear fold in a quartz vein. Minor-scale S-C fabrics are also prevalent and both represent dextral shearing.

3.b Minor-scale asymmetric shear fold within a quartzofeldspathic layer. Asymmetry of fold consistent with dextral shearing.

3.c Minor-scale F_3 fold transected by an apparent minor-scale reverse fault. Thrust plane parallel to bedding planes on the western limb of the fold (to the right of the photo).

3.d Slickenside lineations formed on a quartz vein. Indicate the displacement orientation. 'Step' analysis of slickensides, along with dextral shear indicators, interpret the displacement direction to be up plunge.

3.e Rotated garnet porphyroblast containing a chlorite and muscovite pressure shadow, within the Garnet-chlorite Schist unit. Consistent with dextral shearing.

3.f Chlorite and muscovite pressure shadow of a magnetite porphyroblast, within the Garnet-chlorite Schist unit. Represents dextral shearing.

3.g Microscopic S-C fabric preserved by chlorite and muscovite within the Garnet-chlorite Schist unit. Indicates dextral shearing.

3.h Elongate aggregates of recrystallised quartz minerals defining the S_4 fabric along with chlorite and muscovite within the Retrograde Schist unit.

* lens cap is 55mm in diameter; 'Max' is 30mm in width.

CHAPTER 1 - Introduction

1.1 Introduction

The Weekeroo inliers are situated approximately 150km WSW of Broken Hill, NSW, and are found within the Olary Domain of the Willyama Complex (Figure 1.1). A geophysical and geographic boundary, defined near the South Australia and New South Wales border, separates the western 'Olary Domain' (OD) of the Willyama Complex, from the eastern 'Broken Hill Domain' (BHD) (Ashley *et al*., 1997).

The geological history and evolution of the Willyama Complex, has long been the focus of detailed studies (Ashley *et al*., 1997). The Weekeroo inliers (Figure 1.1) are isolated inliers of this Complex (Berry *et al*., 1978), and may provide invaluable evidence for its geological history.

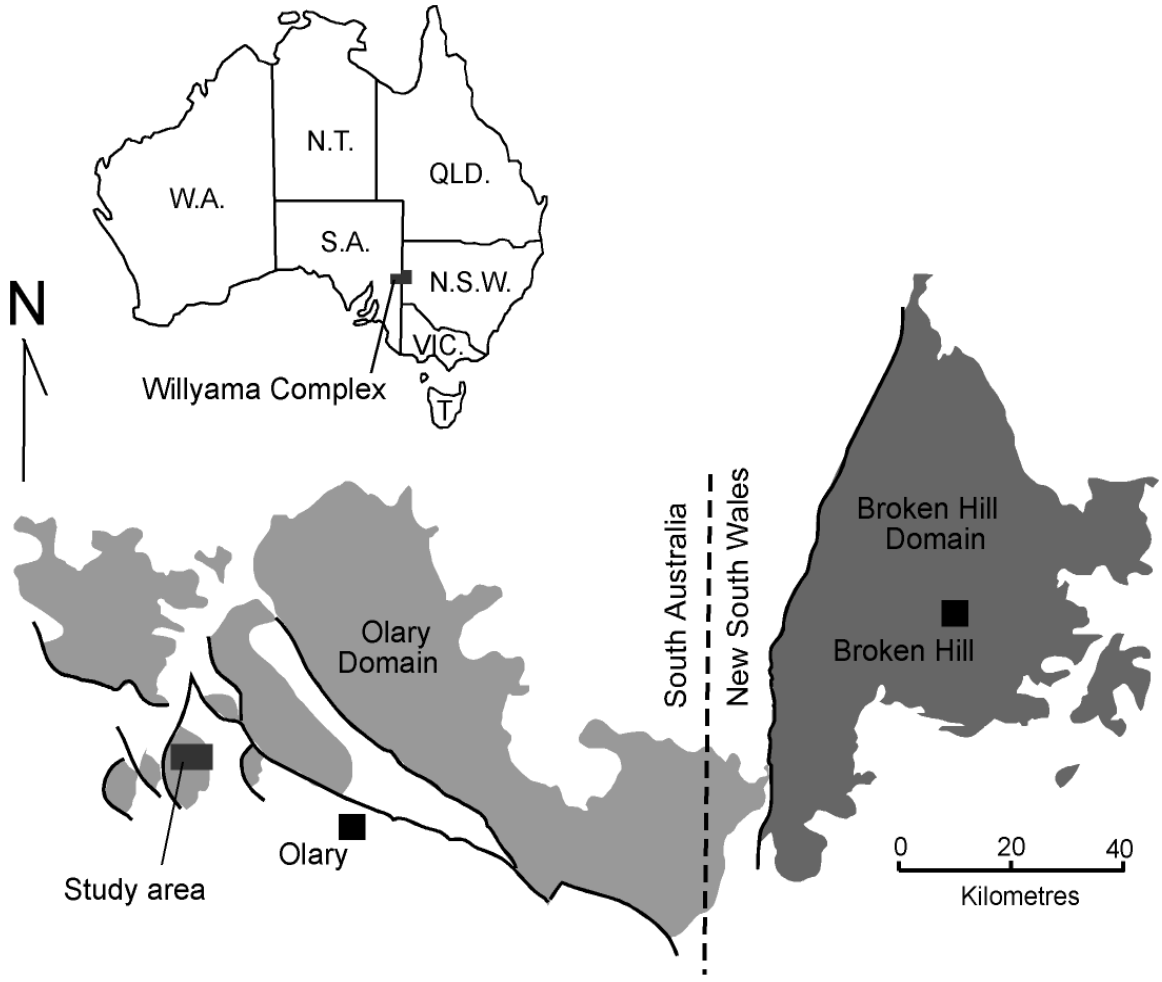

Figure 1.1 Location of the Willyama Complex and study area within the eastern Weekeroo inlier.

The Walter-Outalpa shear zone lies within the eastern Weekeroo inlier. This shear zone represents a prominent feature on magnetic (Figure 1.2) and radiometric imagery. An understanding of the shear zone is important for stratigraphic and structural analysis of the Weekeroo inliers. It is also important for analogy with other basement shear zones of the Willyama Complex. The Willyama Complex is transected by many major shear zones, which influence major mineralisation (eg. Broken Hill mineralisation: Vernon and Ransom, 1971; White Dam mineralisation).

While shear zones within the BHD have been relatively well documented, very little work has been undertaken on shear zones within the OD. The Walter-Outalpa shear zone therefore offers an important example for analysis, and understanding of the shear zones within the OD.

1.2 Review of geometry and kinematics of shear zones in high grade gneiss terrains

Shear zones (Plate 1.a) are localised areas of intense shear strain (Ramsay and Graham, 1970). Displacement in a shear zone is a cumulative effect where total displacement involves an accumulation of movement over a zone of smaller displacements along numerous individual shear planes. This distinguishes shear zones from faults where the entire displacement is accommodated for on a single fault plane. McClay (1987) characterised ductile shear zones by high shear strains, strong foliation development, and large displacements (relative to their widths). Stevens (1986), when studying BHD shear zones, reported that displacement within ductile shear zones is achieved by folding, attenuation, and transposition commonly with boudinage.

Shear zones are usually sites of continuous and progressive increase in shear strain from the shear zone boundary to the centre of the shear zone, where the most highly strained rocks are located (Tourigny & Tremblay, 1997). This variation in intensity of shear strain causes the formation of many different structures, fabrics, and folds (eg. asymmetric porphyroclasts, rotated porphyroblasts etc.). The development and character of any individual structure is particularly dependent upon the amount of strain, the initial morphology of the object to be strained, the competency of the object, the initial orientation of the object to the principal strain direction, and *time* (Hanmer and Passchier, 1991).

Shear zone structures may provide important evidence for the geometrical and kinematic interpretation of a shear zone. These structures are visible on all scales and allow very detailed analysis of shear zones. Ductile deformation and brittle deformation cause very

FIGURE 1.2 Magnetic image of the Walter-Outalpa shear zone and surrounding Gneiss Complex within the central part of the Eastern Weekeroo Inlier.

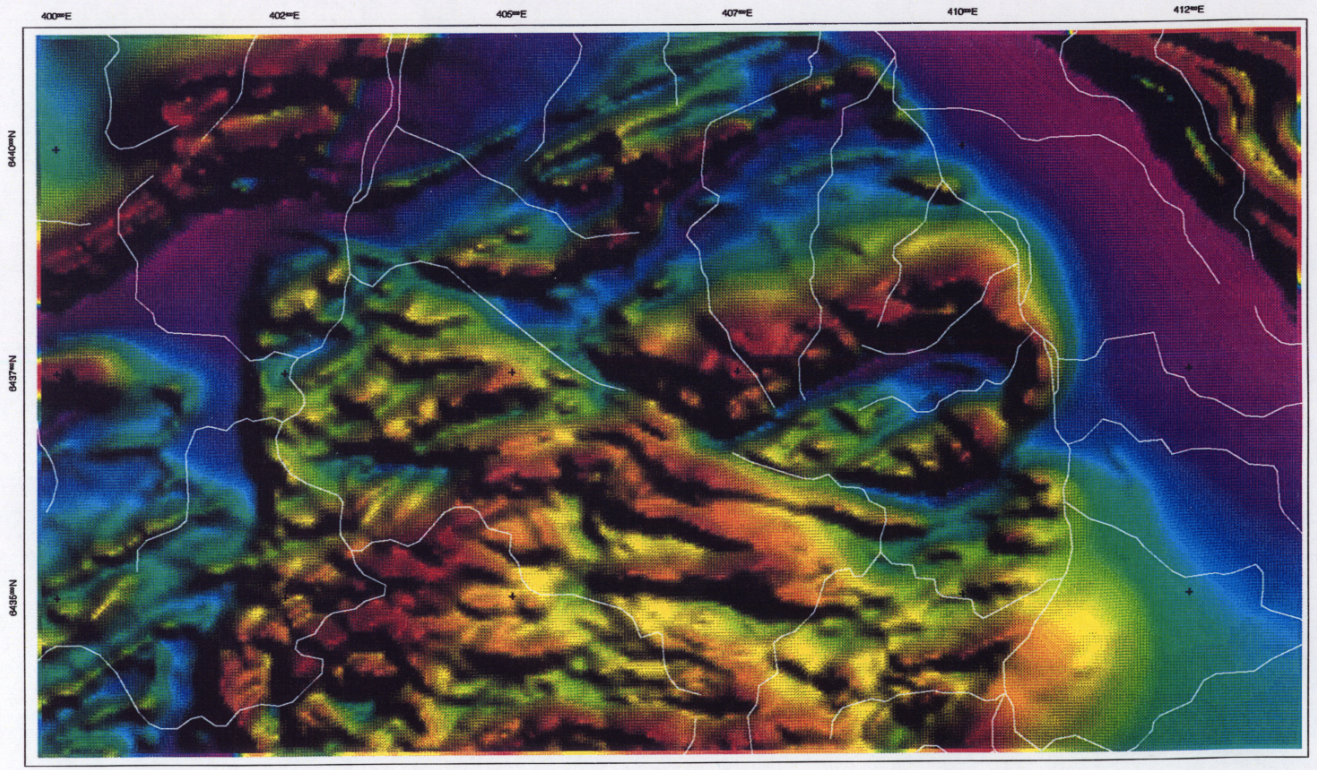

FIGURE 1.2 Magnetic image of the Walter-Outalpa shear zone and surrounding Gneiss Complex within the central part of the Eastern Weekeroo Inlier.

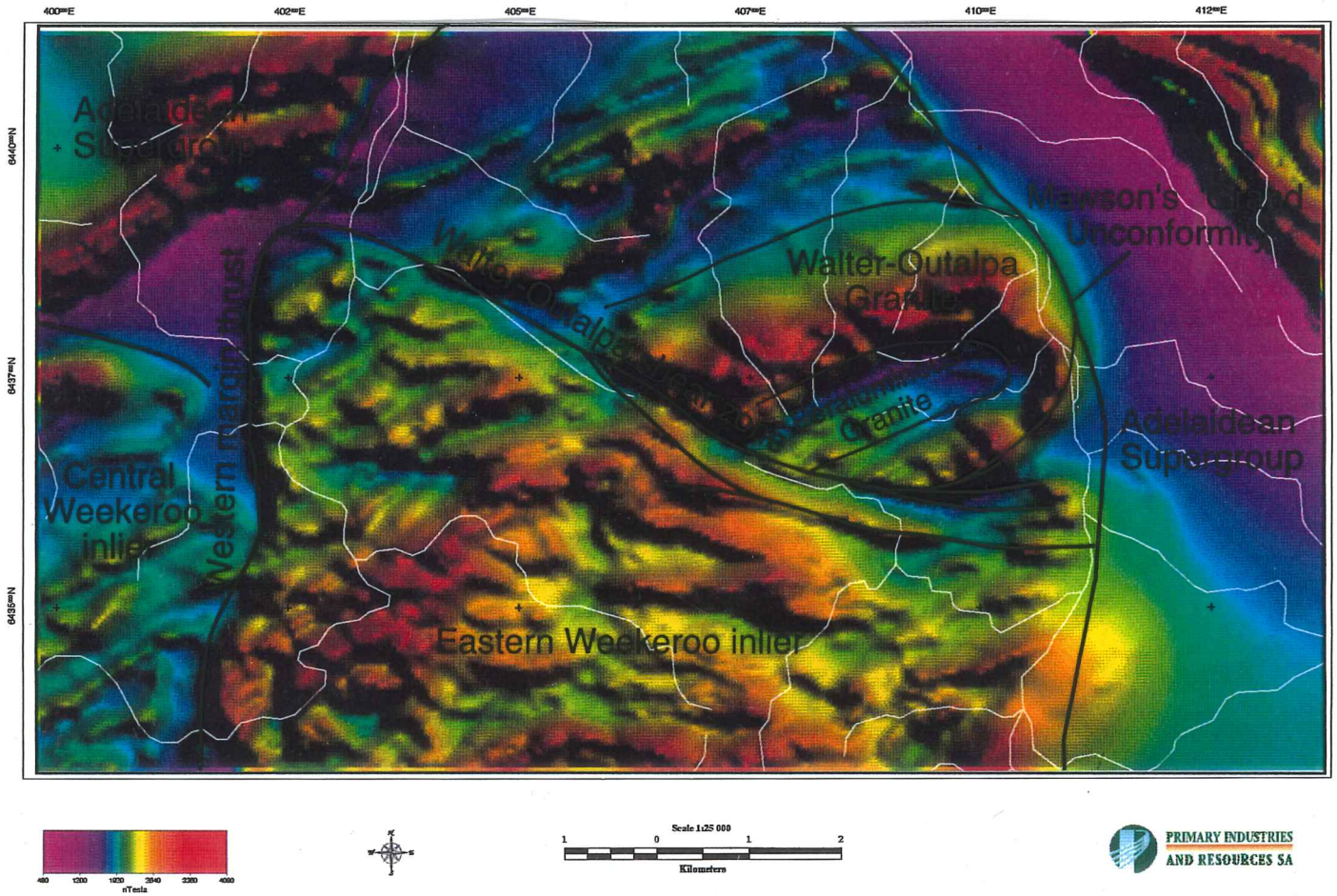

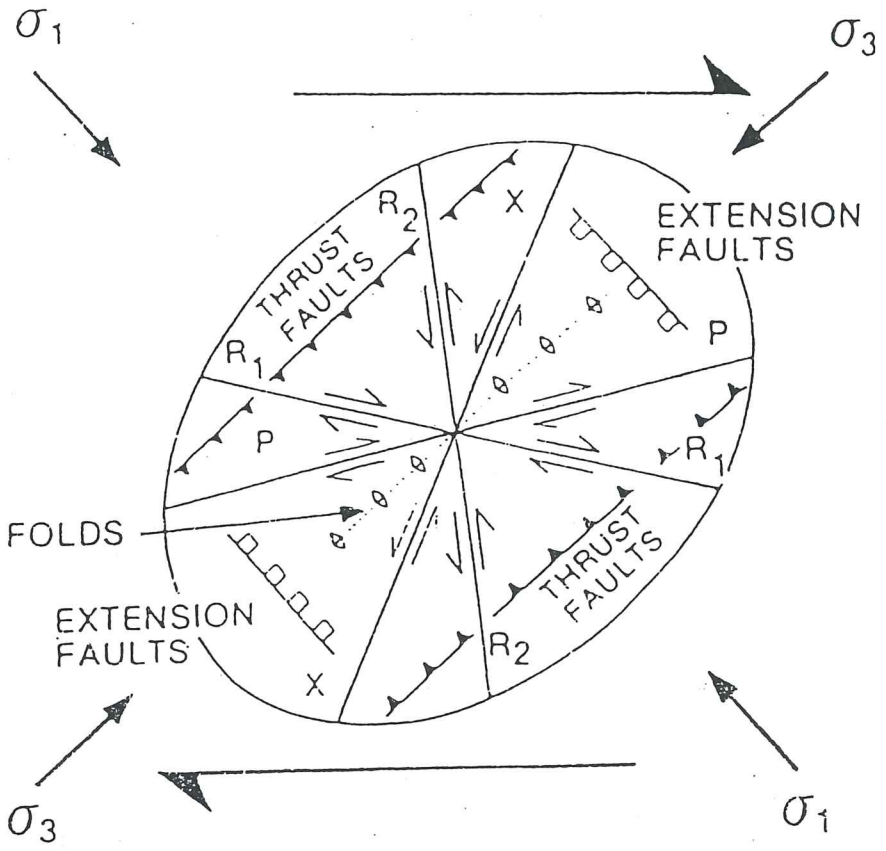

Figure 1.3 Strain ellipse and minor structures found in shear zones (from McClay, 1987).

different, but kinematically related, structures.

Ductile deformation is commonly the most noticeable type of deformation in shear zones. While seen on all scales, it is most readily seen on the minor-scale, at the outcrop level. Important ductile structures include S-C fabrics, asymmetric porphyroclasts, shear zone related folding, boudinage structures, extensional crenulation cleavages (ECC's), and mylonitic fabrics (Hanmer and Passchier, 1991).

Brittle deformation is also very important in shear zones, dominantly in lithologies that have high competency (eg. pelites often deform in a ductile state while directly adjacent psammites can deform in a brittle state) or suffer brittle shear failure. Two types of brittle shear fracture are readily visible in shear zones (Tchalenko, 1970; Biddle and Christie-Blick, 1985). The first shows a synthetic movement sense to the overall displacement of the shear zone occurring along *riedel* fault planes (Figure 1.3, Plate 1.b). The second shows antithetic movement sense to the overall displacement of the shear zone forming *anti-riedel* fault planes (Figure 1.3, Plate 1.c).

Shear zones also act as foci for hydrothermal fluids (Ashley *et al.*, 1997). It is for this reason that retrograde hydrous mineral assemblages occur, as element rich fluids enhance

Plate 1

1.a Minor-scale shear band which displays localisation of shear strain, typical of shear zones. Broken up quartz veins within the shear band show that there is also localisation of hydrothermal fluids.

1.b Minor-scale riedel shear planes transecting and offsetting the more competent quartzofeldspathic layers. Mica-rich interlayers preserve more ductile deformation. Indicates dextral shearing.

1.c Minor-scale anti-riedel shear planes transecting and offsetting a pegmatitic intrusion into the Layered Gneiss unit. Indicates dextral shearing.

1.d Typical appearance of the Migmatitic Gneiss unit on a freshly exposed surface.

1.e Layer parallel (S_1) fabric within the IPMS unit. The black pen defines the strike of the S_1 fabric. The yellow pencil defines the strike of a weak S_2 fabric.

1.f Remnant original layering preserved within calc-silicate.

1.g Typical appearance of the Layered Gneiss unit on a freshly exposed surface.

* lens cap 55mm in diameter

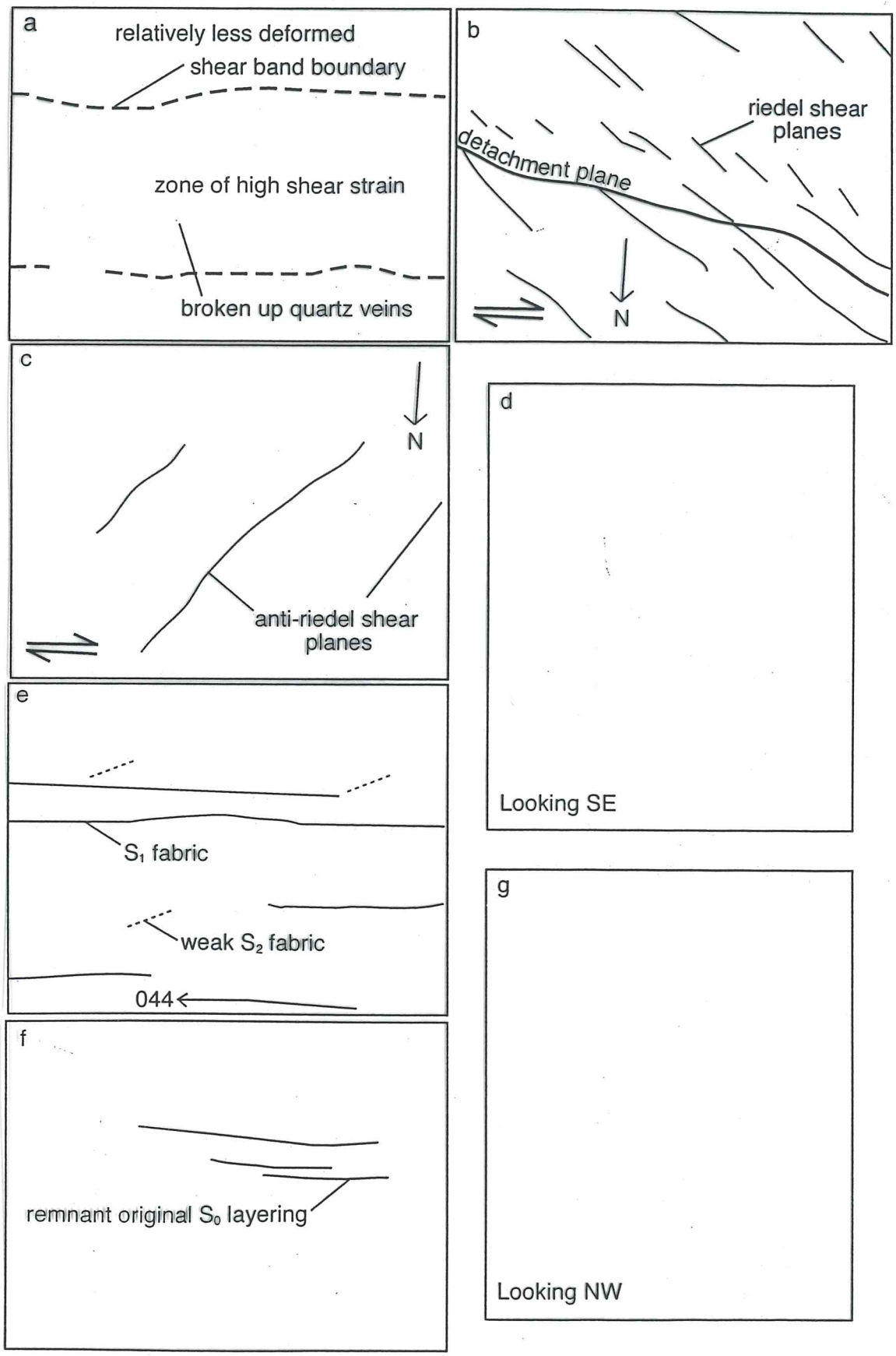
a
relatively less deformed
shear band boundary
zone of high shear strain
broken up quartz veins
b
riedel shear planes
detachment plane
N
c
N
anti-riedel shear planes
d
Looking SE
e
S1 fabric
weak S2 fabric
044
f
remnant original S0 layering
g
Looking NW

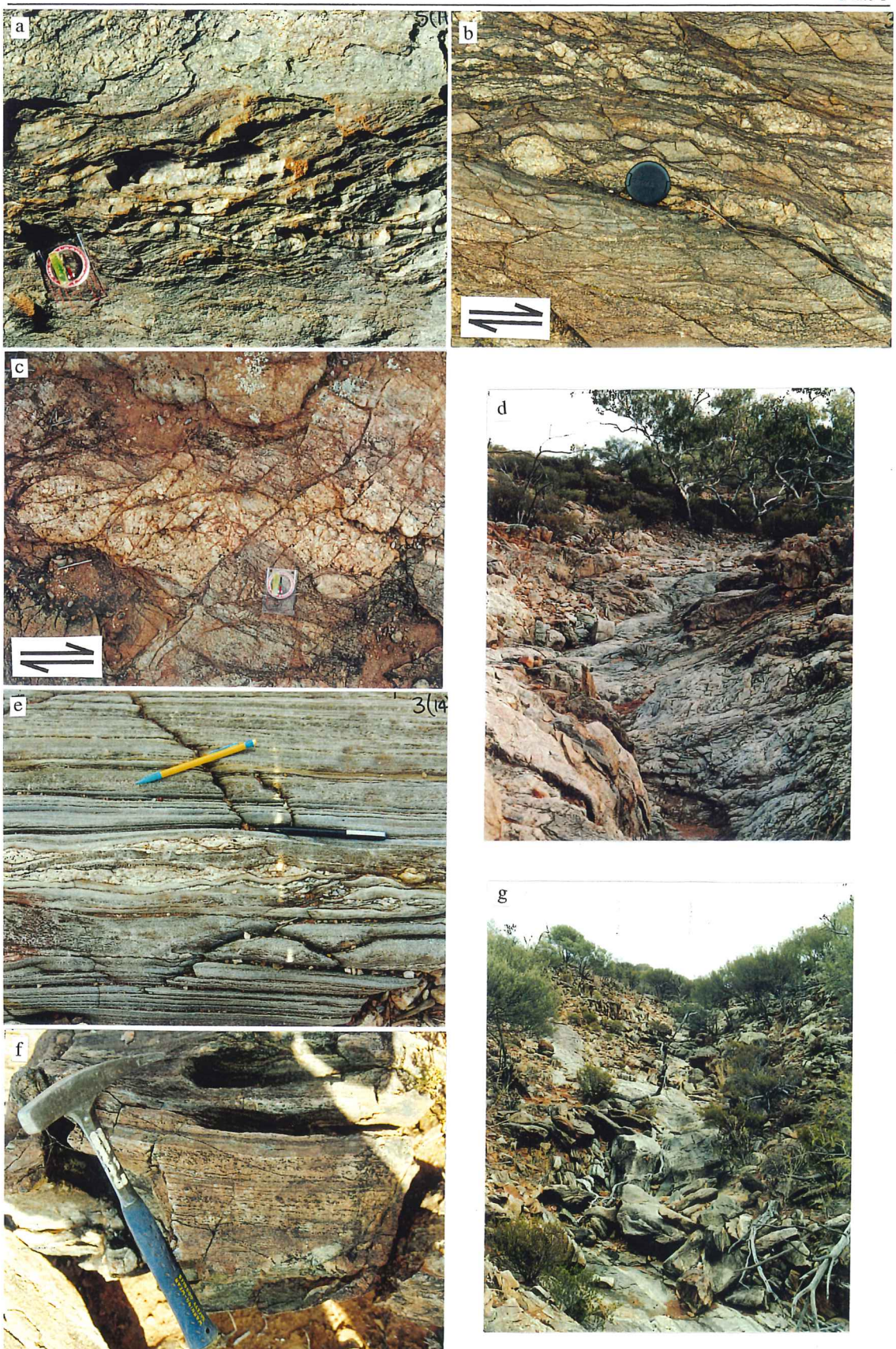
a
5(R
b
c
d
e
3(14
f
g

recrystallisation (eg. chlorite and muscovite). The presence of these fluids also allows for mobilisation of metal elements. Shear zones therefore may act as important sites for mineralisation of the relatively mobile metals.

The Walter-Outalpa shear zone contains both brittle and ductile structures, which are discussed in Chapter 5. These structures represent the end member products of shearing over a long time period, during which the shear zone may have become periodically reactivated. Of importance to this study is the geometry and kinematics of the shear zone based on its varied structures, and the possible strain orientations and history of the shear zone, including estimations on offset.

1.3 Aims of Study

The aims of this study are summarised below;

- To produce a detailed structural map of the area adjacent to and within the Walter-Outalpa shear zone.
- To carry out structural analysis of major and minor structures and fabrics from areas adjacent to and within the shear zone.
- To use microstructures and kinematic indicators to outline the geometry and evolution of the shear zone.
- To apply Sm-Nd geochronological techniques in order to date movement of the shear zone. Assuming metamorphic assemblages relate to main shear zone activation.
- To use this evidence as further information for current tectonic models and dating of regional retrograde shear zone formation, and finally to compare the Walter-Outalpa shear zone with other related shear zones in the Olary and Broken Hill Domains.

1.4 Methods

A major part of this study involved mapping the Walter-Outalpa shear zone in the central part of the eastern Weekeroo inlier. This mapping was undertaken over a six week period beginning on the 20th of April, and concluding on the 1st of July, 1998. Mapping involved identifying lithological boundaries and, in particular, zones of intense shearing. In addition, structural data was collected on fabrics, folds, oriented hand specimens, and kinematic indicators etc. Thin sections were cut from selected samples for mineralogical and structural descriptions.

Mapping was undertaken on aerial photographs obtained from the Department of Primary Industries and Resources of South Australia. Photographs (1:25,000) were rescaled to approximately 1:10,000 to aid with mapping at an appropriate scale. Photo interpretation was used as a guide for mapping of the shear zone. Maps were drafted later using the computer drafting program, *Freehand*©.

Garnet bearing schists were collected at selected sites during fieldwork along the Walter-Outalpa shear zone. Garnet along with chlorite, muscovite, and biotite, enabled Sm-Nd dating of one of these rocks in an attempt to find the age of the main phase of movement along the shear zone.

Data from the field, hand specimens, and thin sections, allowed structural analysis to be undertaken. This consisted of describing and measuring major and minor structures to enable analysis of folds, fabrics, offset, and shear zone kinematics. An important tool for this analysis was the *stereoplot*© computer program.

CHAPTER 2 – Regional Geology of the Olary Domain

2.1 Previous Research

The geology of the Willyama Complex has been well studied (Ashley *et al*., 1997). However there is little detailed work on the OD. Studies undertaken previously involved local mapping and research, which led to a regional synthesis of lithological variation into a stratigraphic framework (eg. Campana and King, 1958). This was further investigated by Clarke *et al*. (1986) and more recently Ashley *et al*. (1997; 1998). This accompanied work by others into the deformational history of the OD (eg. Talbot, 1967). Berry *et al*. (1978) undertook a major deformation study into the Outalpa area, including part of the Weekeroo inliers. Forbes and Pitt (1980) also made a study into the deformation history, however the most recent and detailed work has been documented by Ashley *et al*. (1997; 1998). This represents a collation of all OD analyses to date, including much unpublished work carried out through the former Department of Mines and Energy of South Australia. Clarke *et al*. (1987) documented metamorphic assemblages within the OD, and later Clarke *et al*. (1995) studied in particular retrograde metamorphic assemblages such as staurolite + chlorite + muscovite.

Significant mapping programs, by exploration companies and university Honours projects (eg. ESSO, The University of Adelaide, and Flinders University), have been carried out in much of the OD, including the Weekeroo inliers of this study. An overview of this regional work has led to the stratigraphic and structural interpretations outlined in this chapter.

2.2 Stratigraphy of the Olary Domain

Two major groups of metasediments are represented within the OD. The oldest group is the Palaeoproterozoic Willyama Supergroup, which is unconformably overlain by the upper Proterozoic Adelaidean Supergroup.

2.2.1 Willyama Supergroup

The Willyama Supergroup has been divided into five main suites, composed primarily of migmatitic and metasedimentary gneisses and schists. Metasediments were deposited in varied environments, ranging from deep water to evaporitic. Willis *et al*. (1983) and other authors have broadly correlated the Olary Domain lithogies with the Willyama

Supergroup of the Broken Hill Domain (Figure 2.1). The five OD suites comprise as follows:

Composite Gneiss Suite (CGS)

Clarke *et al*. (1986) interpreted this as the basal unit of the Willyama Complex. It is a coarse-grained quartz - feldspar - biotite ± sillimanite ± garnet gneiss of primarily metasedimentary origin (Ashley *et al*., 1997). Ashley *et al*. (1997) state that the CGS is currently interpreted as simply the lower part of the overlying Quartzofeldspathic Suite that experienced a higher degree of anatectic melting.

Quartzofeldspathic Suite (QFS)

The QFS is composed of quartz - plagioclase gneisses and quartzites. It is subdivided into three units. The "Lower Albite" member is represented by leucocratic granitic gneiss. Locally intervening "Middle Schist" was deposited in deep water and comprises psammopelitic schist and composite gneiss (Ashley *et al*., 1997). The "Upper Albite" member is composed of metasedimentary gneisses possibly sourced by felsic igneous rocks based on work by Page and Laing (1992).

Calcsilicate Suite

This is a massive to finely laminated suite made up of calcsilicates and quartzofeldspathic rocks. Ashley *et al*. (1997) proposed an evaporitic origin for this suite. The presence of stratabound breccia masses widely distributed throughout the Olary Domain is an important marker of this unit (Ashley *et al*., 1997).

Bimba Suite

This suite is made up of quartz - albite - biotite meta-siltstones hosting pyritic sulphides. The Bimba suite is only thin (<50m), but remains continuous through the central and northern parts of the Olary Domain (Ashley *et al*., 1997).

Pelite Suite

This is a biotite - muscovite ± Al silicate unit of pelitic and psammopelitic schists. Ashley *et al*. (1997) described the Pelite Suite as indicating a deepening marine environment. The top of the Pelite Suite is not exposed within the Olary Domain.

Intruding all Willyama Supergroup rocks are two granitoid types. A-type granites believed to be emplaced around 1700 Ma (Glen et al., 1977) are further intruded by S-type granites emplaced around 1590 Ma (Ashley *et al.*, 1997).

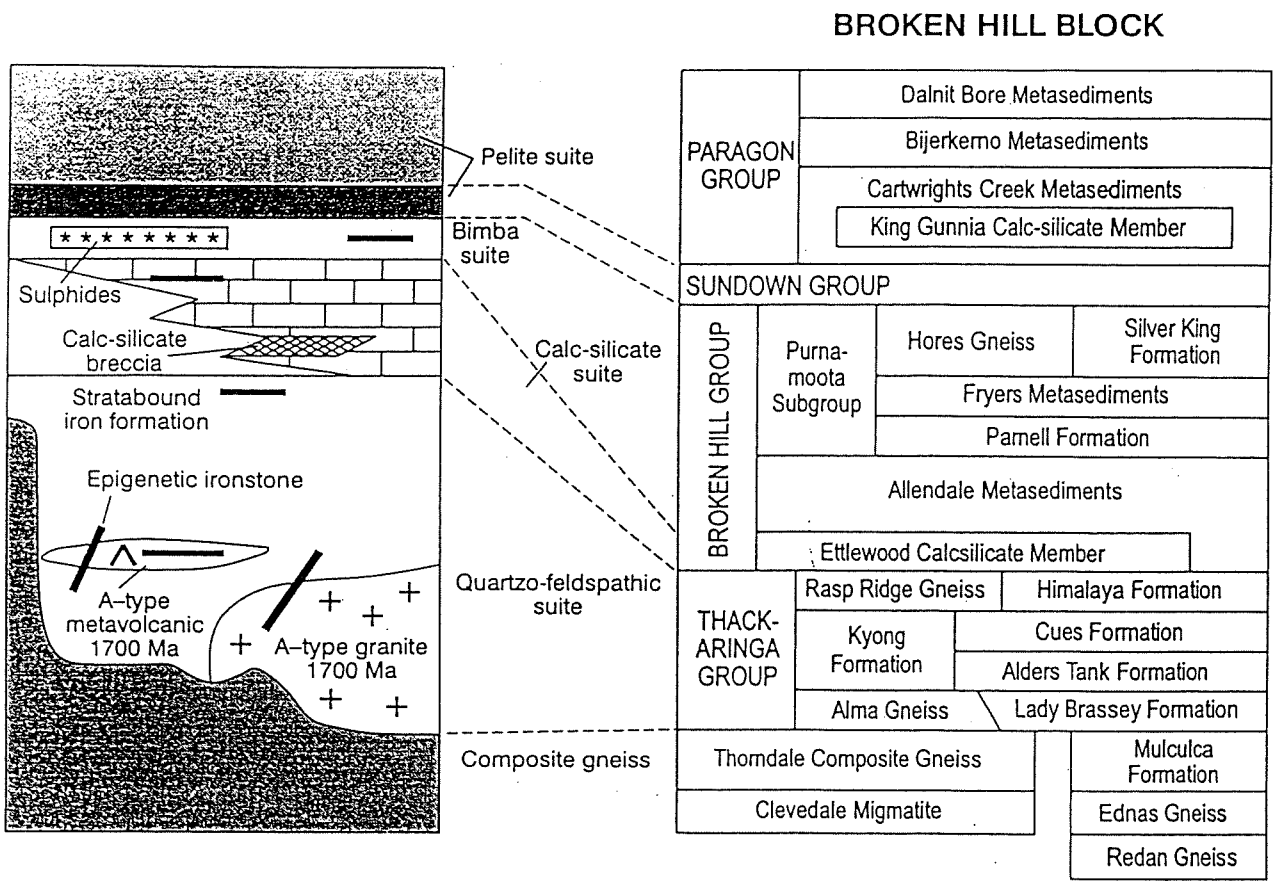

Figure 2.1 Interpreted stratigraphic correlation between the Olary and Broken Hill Domains (Ashley *et al.*, 1998).

2.2.2 Adelaidean Supergroup

The Adelaidean Supergroup is composed of metasedimentary quartzites, siltstones, and conglomerates. The Burra Group consists of the earliest Adelaidean metasediments and is in unconformable contact with the Willyama Supergroup (Ashley *et al.*, 1997). The most basal unit of this group is a thin conglomerate. This serves as a marker bed for the boundary between the two Supergroups. Quartzites and siltstones make up the upper portions of the Burra Group, which contacts with the overlying Umberatana Group.

2.3 Deformation History

The Willyama Complex has undergone two major periods of deformation (Figure 2.2). The earliest deformation period occurred during the Palaeoproterozoic, and is known as the Olarian deformation. Retrograde shear zones are a late stage process of this. Clarke *et al.* (1987) attributed movement on these pre-Adelaidean retrograde shear zones to the presence, and outcrop pattern of the Olary Domain at its present day erosional surface. The Delamerian Orogeny caused the second major deformation period, which occurred during Cambro-Ordovician time.

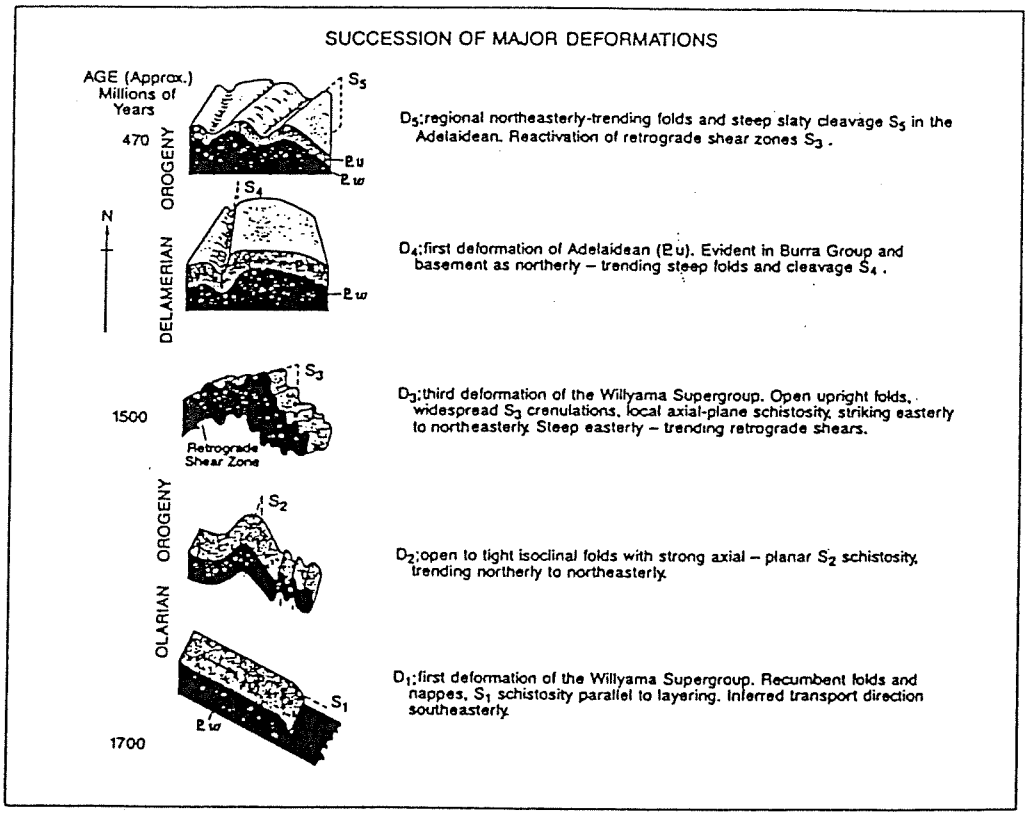

Figure 2.2 Interpreted succession of major deformation events for the Olary Domain (Forbes, 1991).

2.3.1 Olarian Deformation (OD_1, OD_2, and OD_3)

The number of discrete Olarian deformation phases observed within the Willyama Complex varies depending upon individual interpretation. Berry *et al.* (1978), Forbes and Pitt (1980), and Ashley *et al.* (1997; 1998), describe three phases of deformation during this Palaeoproterozoic Olarian Orogeny (Figure 2.2).

OD_1, the first Olarian deformation, is interpreted as recumbent folds and nappes (Forbes, 1991), inferring a southeasterly transport direction. Major F_1 folds are interpreted

from reversals of structural facing of bedding and fold analysis. S_1 schistosity is parallel to original layering (S_0).

OD_2 has a strong axial-planar S_2 schistosity trending northerly to northeasterly (Forbes and Pitt, 1980). F_2 folds are open to tight isoclinal folds which may be misinterpreted from refolded F_1 folds.

OD_3 includes open upright F_3 folding and widespread S_3 crenulations. Local axial-planar schistosity strikes easterly to northeasterly (Forbes, 1991). Steep retrograde shear zones, related to the Walter-Outalpa shear zone, trend easterly. They are regarded as a late stage process of *O*D_3 (Ashley *et al*., 1997; Glen *et al*., 1977; Clarke *et al*., 1986).

Talbot (1967) and later Clarke *et al*. (1986) describe only two pervasive deformations. The *O*D_2 and *O*D_3 phases of Berry *et al*. (1978) are combined as a continuous deformational event rather than two discrete deformation periods.

2.3.2 Basement Shear Zones (Late stage *O*D_3)

Ashley *et al*. (1997) recorded that Proterozoic retrograde shear zones seem to crosscut all Willyama Supergroup rock types and Mesoproterozoic intrusives. Several trends of retrograde shear zones have been noted with E-ENE, NE, and NW being the most prominent.

It is important to distinguish Cambro-Ordovician shear zones near the margins of the Willyama Complex from pre-Adelaidean retrograde shear zones. Clarke *et al*. (1986) distinguish these by the presence of sheared Adelaidean pebble clasts within presumably Cambro-Ordovician shear zones. Shearing of the basal unit of the Adelaidean in contact with the Willyama lithologies, however, can be a result of basement shear zones. This is due to re-activation of Olarian shear zones during the Delamerian.

In contrast to the Olary Domain, retrograde shear zones in the Broken Hill Domain have been well studied (Hobbs, 1966; Hobbs and Vernon, 1967; Williams, 1967; Ransom, 1968; Vernon and Ransom, 1971; Etheridge and Cooper, 1981; AGSO, 1997). Broken Hill Domain shear zones, which may be analogous to the Olary Domain shear zones, exhibit steeply dipping foliation orientations and steeply-plunging lineations (Vernon and Ransom, 1971). The foliation is usually parallel to the edges of the shear zones (Vernon and Ransom, 1971), overprinting all earlier formed fabrics.

Some radiometric dating of retrograde shear zones has been carried out in the Broken Hill Domain. Evernden and Richards (1961), and Richards and Pidgeon (1963), used K/Ar and Rb/Sr mineral dating techniques to record a late retrogressive Delamerian event at

approximately 500 Ma. Binns and Miller (1963) suggested a possible event at 800Ma based on K/Ar dating, however no further confirmation of this has been published.

2.3.3 Delamerian Deformation (*D*D$_1$ and *D*D$_2$)

The overlying Adelaidean sequence contains evidence of two deformations (Figure 2.2). *D*D$_1$ is the first of the Delamerian deformations, and consists of upright folds trending northerly, as does the cleavage. Thrusting on the western margins of Willyama Supergroup inliers, such as the Weekeroo inliers, is synchronous with *D*D$_1$.

*D*D$_2$ folds have a steeply dipping slaty S$_5$ cleavage within the Adelaidean, resulting from northeasterly trending *D*F$_2$ folds. *D*D$_2$ folds and *O*D$_3$ folds may be confused as Flint and Parker (1993) noted that they both contained retrogressive assemblages and have folds trending in the same orientation (east to northeast).

Little overprinting of the Willyama Complex results from the Delamerian events (Clarke *et al*., 1986). Much of this overprint is shown within reactivated and post-*O*D$_3$ shear zones. Shearing in the basal conglomerate of the Adelaidean sequence where basement shear zones terminate represents reactivation of the Olarian retrograde shear zones. Moderately intense folding in basal Adelaidean sequences where basement shear zones terminate are in many cases also related to Delamerian reactivation (Glen *et al*., 1977). Reactivation of *O*D$_3$ retrograde shear zones is reported to be synchronous with *D*D$_2$ (Ashley *et al*., 1997).

2.4 Metamorphic History

The general metamorphic history of the Willyama Supergroup implies an anti-clockwise pressure-temperature-time path (Clarke *et al*., 1987). This is seen with *O*D$_1$ and *O*D$_2$ representing progressive metamorphism to mid-amphibolite facies (Figure 2.3). *O*D$_3$ (Berry *et al*., 1978) shows retrogression from amphibolite facies to greenschist facies. This was adjusted by Clarke *et al*. (1986) who recognised only two Olarian deformation events. *O*D$_1$ remains a progressive deformational event to mid-amphibolite facies. *O*D$_2$ however represents the transition to retrograde greenschist facies metamorphism. The two Cambro-Ordovician Delamerian deformations (*D*D$_4$ and *D*D$_5$) occurred under upper-greenschist facies metamorphism.

The Olary Domain has been divided into metamorphic zones according to mineral assemblages (Figure 2.4). The Weekeroo inliers are collectively grouped into the IIb metamorphic zone after Clarke *et al*. (1987). Andalusite and staurolite are the prominent metamorphic porphyroblasts represented throughout this group IIb zone.

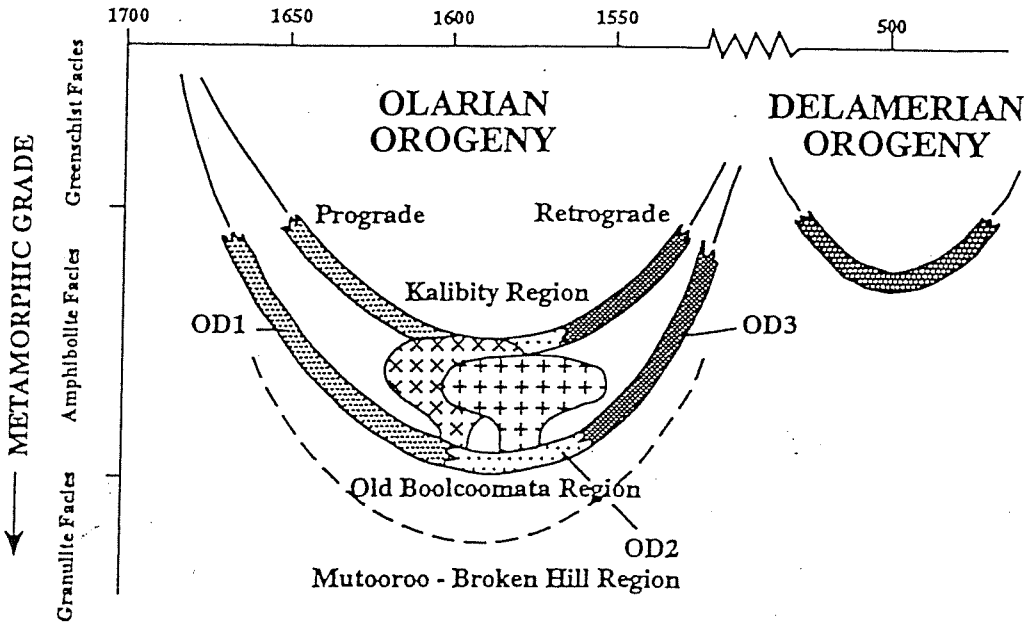

Figure 2.3 Timing and metamorphic grade of the Olarian and Delamerian deformational events (Flint and Parker, 1993).

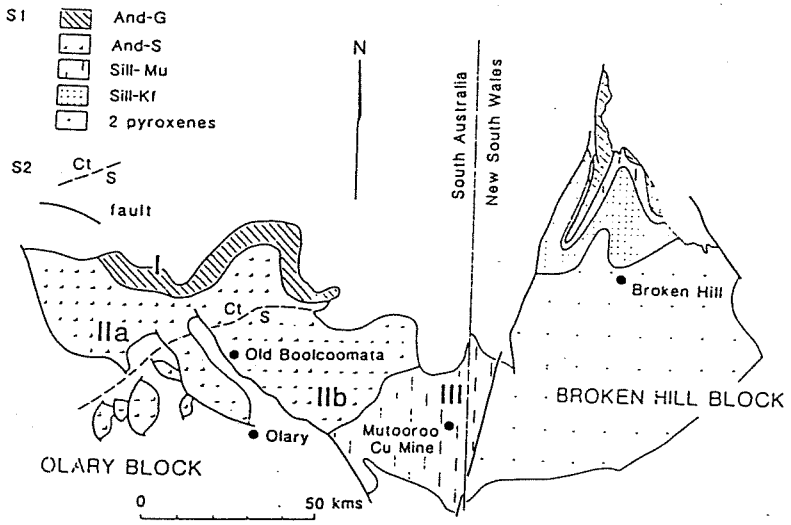

Figure 2.4 Metamorphic Porphyroblast assemblages through the Olary and Broken Hill Domains (Clarke *et al.*, 1987).

CHAPTER 3 – Lithological Variation of Gneiss Complex and Shear Zone of the eastern Weekeroo inlier

3.1 Introduction

Lithologies from within the Walter-Outalpa shear zone are significantly different from lithologies found outside of the shear zone, which are referred to here as the Gneiss Complex (GC). GC lithologies are much less deformed than shear zones lithologies (SZ), and they also show higher grade mineral assemblages. The GC is composed of metasedimentary and granitic gneisses, both of which show evidence of tectonothermal fabrics. The SZ are composed of schists and gneisses. Schists commonly show more ductile shearing whereas gneisses record both ductile and brittle shearing.

Lithologies discussed during this chapter relate to the map (Figure 3.1) drafted for this study. Lithological naming of local lithologies has not been related to the lithological suites documented for the OD (Ashley *et al*., 1997; 1998).

3.2 Field distribution and relationships between Gneiss Complex and Walter-Outalpa shear zone lithologies

The position of lithological units within the mapping area is partially dependent upon the effects of the Walter-Outalpa shear zone (Figure 3.1). Related units on the southern side of the shear zone are interpreted to be set further westward than their northern counterparts. Units to the north of the shear zone represent a continuously northwestward younging stratigraphy. The repetition of the Andalusite Schist unit in the NW of the mapping area may represent opposed limbs of a possible F_1 isoclinal fold (Chapter 4.2, First Deformation). The discontinuous calc-silicate and mica schist unit represents the youngest unit of this stratigraphy.

All GC units have been sheared and dextrally displaced by the shear zone. Only one unit of the GC may be recognised on both sides of the Walter-Outalpa shear zone. The Walter-Outalpa Granite (Brett, 1998) can be traced, through the shear zone, to the southern side (Western Granite Sheet; Figure 3.1). The Migmatitic unit surrounds the Western Granite Sheet within the mapping area, which Brett (1998) has indicated isotopically relates to the Walter-Outalpa Granite. Migmatitic Gneiss dominates the stratigraphy south of the shear zone. The Migmatitic Gneiss on the southern side, is situated stratigraphically equivalent to

Central, Eastern Weekeroo Inlier

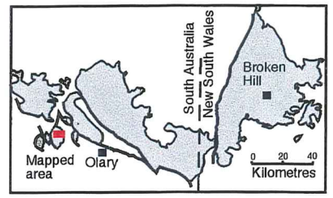

140°00'00"

404000 405000 406000 407000 408000 409000 410000 411000

6439000 6438000 6437000 6436000

Index of adjoining 1:250 000 map sheets

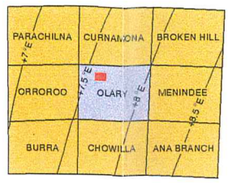

showing magnetic declination

Alluvium

U/C

Adelaidean metasediments

U/C

Amphibolite

Pegmatite

Eastern quartzofeldspathic gneiss (EQG)

'Quartz eye' bearing quartzofeldspathic gneiss (QE)

Layered gneiss with some migmitisation, and LG with thick quartzite bands (LG)

Retrograde schist (RS)

Peraluminous granite (PG)

Walter-Outalpa granite (WG)

Migmatitic gneiss (MG)

Discontinuous calc-silicate and mica schist, cummingtonite layers

Andalusite schist (AS)

Interlayered psammite, quartzite, and mica schist (IPMS)

Western granite sheet

Walter-Outalpa Granite

pinnacles

Au, Cu
Walter Outalpa Mine

Weekeroo Mine
Ba

23	layer parallel foliation (S_1)		lithological boundary
35	granitic foliation		trend line
45	shear (c) plane (S_4)		fault
11	shear lineation		creek
70	minor overturned syncline	gt	garnet-chlorite schist
54	minor synform		protomylonitic ductile shear fabric
67	minor antiform		quartz pods
	younging		mine (abandoned)
		f	fault gouge

TN MN 8°

SCALE

metres 200 0 200 400 600 800 1000 metres

Drafted by Anthony Bottrill B. Sc.
Department of Geology and Geophysics
The University of Adelaide, 1998

Australian Mapping Grid SI - 54 - 2

Figure 3.1 Map of the Walter-Outalpa shear zone

that of the Peraluminous Granite which occupies the northern side. The fact that the Peraluminous Granite (PG) is not present on the southern side may relate to its intrusive character. The stratigraphic contacts of the PG to the east and west indicate an intrusive contact with surrounding units. The boundary between the Migmatitic Gneiss and the Layered Gneiss is notably related to shearing, as are all boundaries of the SZ.

The Layered Gneiss unit is sheared into the shear zone from the SE. Other Shear Zone lithologies however, have unknown lithological parents. Two quartzofeldspathic gneiss units are found entirely bounded by the shear zone and cannot be related to any lithologies visible within the outside Gneiss Complex. The Gneiss Complex parent of the Eastern Quartzofeldspathic Gneiss unit is covered by Adelaidean Supergroup sediments. The Retrograde Schist unit displays the most prominent shear fabric within the SZ, and represents zones of localised intense ductile protomylonitic shearing. They are present throughout the shear zone however they are usually less than 2m wide. Near the eastern margin of the Walter-Outalpa shear zone, the Retrograde Schists are up to 40m wide.

3.3 Lithological and Petrological Description

The GC represents the regional lithological variations of the basement inliers. SZ are confined to more localised areas which contain intense deformation. GC show evidence of all Olarian deformations, whereas SZ show some early deformation, however shearing overprints the majority of this. Amphibolites and pegmatites are found within both major lithological groups.

3.3.1 Gneiss complex lithologies

Migmatitic gneiss (MG)

The migmatitic gneiss (Plate 1.d) is located by low undulating hills within the mapping area. Outcrops are mostly massive and rounded in appearance. A strong layering is evident, with pegmatitic units prevalent, especially close (within tens of metres) to the shear zone.

The migmatitic gneiss shows a high (40%) melt fraction. Both felsic and mafic igneous intrusions are present within the MG, along with psammitic and pelitic layers. Mixing of metasedimentary and meta-igneous units is very obvious within this unit. The most dominant minerals include quartz and plagioclase, within psammites, and biotite and

muscovite, within pelites. Sedimentary and igneous layers are often significantly boudinaged and folded.

Walter-Outalpa granite (WG)

The WG is a relatively large homogeneous granitic body. In the field, the WG has a blocky appearance with characteristic quartz augen an important lithological indicator. The WG defines many of the larger hills in the region due to this blocky nature.

The WG contains 50% quartz, which has a bimodal grainsize. Medium sized interlocking quartz grains form a groundmass for larger quartz augen, which reach up to 10mm in size. Plagioclase in the form of albite makes up 30% of the mineralogy, with biotite, which forms the foliation, making up 10%. This foliation, though weak, commonly dips 80º SE striking towards 045°. However this foliation intensity may be variable, depending upon its closeness to the boundary of the metasediments.

Magnetite, which overgrows the three major rock forming minerals, accounts for 5%. The WG displays a high magnetic susceptibility because of this, showing up as a distinct magnetic high body on the 1:25, 000 scale magnetic image (Figure 1.2).

Geochemically the WG displays an A-type character, with high Ga/Al and Zr+Ce+Nb+Y but a low Aluminium Saturation Index (ASI), of the range 1.1 – 1 (Brett, 1998).

Western Granite Sheet (WGS)

Brett (1998) has shown that the WGS is isotopically related to the WG, however their mineralogy is somewhat different. The WGS has a higher plagioclase content than the WG. This plagioclase is strongly sericitised. Plagioclase makes up 45% of this granitic body, equalling the quartz content. Quartz is represented by both undeformed and deformed grains. Deformed grains contain undulose extinction, while undeformed grains have more regular, euhedral boundaries. Quartz and plagioclase, making up the more major phases of the WGS, have equigranular, medium sized grains.

Minor minerals include magnetite, muscovite, biotite, and microcline, with trace amounts of fluorite. Magnetite formed later than the rock forming minerals as a replacement mineral of plagioclase, and especially micas. Muscovite is always found in association with the biotite, and along with magnetite all three define the major foliation.

Magnetite aggregates form the most visible foliation in hand specimen, and makes up 7% of the rock. As with the WG, the foliation of the WGS has a variable trend, from 045° to

090° as it approaches the shear zone where it becomes more intense. This foliation is more penetrative than that visible in the WG.

Peraluminous granite (PG)

The Peraluminous granite (Brett, 1998) which intrudes the A-type WG defines lower rolling hills and plateaus, in distinct geomorphological contrast to the WG defined hills. This sharp boundary is evident on both aerial photographs and magnetic imagery (Figure 1.2). Outcrop of the PG is more readily weathered than the WG and is therefore very friable, with few fresh samples available. The PG shows up much lower magnetically than the WG, due to little or no magnetite presence. Instead biotite makes up the major foliation which is much stronger in this granite than the WG or WGS. Biotite that forms the foliation is very elongate, and varies in intensity and trend.

The two important rock forming minerals are quartz and albite. Both contain inclusions, especially albite. Sericite is a major replacement mineral, especially within albite. Trace amounts of microcline also occur.

Interlayered psammites, quartzites, and mica schists (IPMS)

The IPMS is composed of thin (20mm thick) interlayered units (Plate 1.e). Towards the WG, the IPMS is primarily made up of psammitic and quartzitic layers. As this unit nears the Andalusite Schist however, mica schists become dominant. Reverse graded bedding (from fine-grained quartz to coarse-grained biotite) may be seen through psammitic layering. Grading, that occurs over a distance of approximately 10mm, indicates overturned bedding (Figure 3.1).

Quartz and feldspar are dominant, with high proportions of thin biotite layering, along with some muscovite.

Andalusite schist (AS)

Two AS units are mapped in the NW of the mapping area. Both contain very similar mineralogy, however the northern AS contains larger andalusite porphyroblasts (up to 10cm). Porphyroblasts are made up most prominently of andalusite and some staurolite. A schistose fabric wraps around these porphyroblasts, forming a relatively intense crenulation. Andalusite porphyroblasts within the more northwestern AS may be up to 10cm in width, while those within the southeastern AS tend to be less than 4cm.

The schistosity is primarily composed of muscovite with a large contribution from biotite. Some retrogression of the biotite has caused the formation of chlorite. Quartz is

present in small 'augen shaped' areas between this fabric. Magnetite seems to overgrow all phases, especially the micas.

Clarke *et al*. (1995) have mapped the two AS's as being the same unit on separate limbs of a major-scale anticline. The map within this study also presents them as the same lithological unit (Figure 3.1).

Discontinuous calc-silicate and mica schist

Calc-silicate is very discontinuous within the mapping area, and is interleaved with micaceous schists. Pods of calc-silicate, up to 25m thick and 100m length, terminate abruptly along strike.

The calc-silicate is layered to massive, often showing remnant original bedding (Plate 1.f). Interlayered epidote and actinolite layers, about 30-40mm thick, are prominent. Quartz and feldspar comprise the other mineral phases present. Massive calc-silicate is composed of nodules of particularly epidote (up to 10cm), and bedding is completely obliterated or not present.

Layer-parallel pods (1m × 10m) of the amphibole mineral cummingtonite are also present within the muscovite schists of this unit. Pods generally lie along strike from one another.

3.3.2 Shear zone lithologies

Layered gneiss (LG)

The LG is the most extensive unit of the shear zone lithologies (Plate 1.g), however it is also present within the eastern Gneiss Complex. Psammitic and pelitic layering predominates. Layers are usually around 60mm thick, however layers of much greater thickness are present. Psammitic layers of quartz and plagioclase dominate, and show various brittle shear structures (Chapter 5.2 Structural Interpretation). These structures are also seen in felsic igneous components, which are involved with migmatisation of the unit. Migmatisation of the LG is strong near granite boundaries. There are also minor-scale mafic igneous bodies present within the layered gneiss.

Pelitic layers contain a strong biotite, chlorite, and muscovite fabric. Shear bands through this lithology are generally less than 2m thick, and strongly schistose. The far SE corner of the mapping area, south of the shear zone, contains a similar lithology, however it contains some thick (4m across) quartzite layers which are not seen in the LG.

Garnet-chlorite schist (GS)

The GS are thin layer-parallel units found within schistose layers or gneiss. Their alteration characteristics make them less affected by weathering than surrounding layers, therefore forming upstanding outcrops up to a metre high. Black staining of these units, probably caused by manganese (Conor pers comm., 1998), makes them very distinctive in the field. Generally these layers are not extensive along strike.

Garnet crystals up to 6mm are abundant within this unit. Microprobe analysis has confirmed them to be almandine garnet. Chlorite is extensive as a retrogressive phase of biotite, however there is still a marked component of biotite. Muscovite is present to a lesser extent and, along with the chlorite and biotite, forms the schistosity. Coarse magnetite minerals are also present. This unit, along with its mineralogy, is further discussed in Chapter 5.2.3, Microstructures.

'Quartz eye' bearing quartzofeldspathic gneiss (QE)

The QE is only manifest within the boundaries of the shear zone, between shear bands. This medium grained lithology contains two distinct quartz sizes. Phenocrysts ('quartz eyes') are very prominent, especially on weathered surfaces. They may show a mineral elongation when close to a shear band. Medium grained quartz clasts constitute the matrix, along with plagioclase, biotite, and muscovite. Chlorite becomes prominent when close to shear bands. This lithology is relatively resistant compared with the schistose lithologies further north, therefore it defines the beginnings of hills to the south of the shear zone.

Eastern quartzofeldspathic gneiss (EQG)

The EQG stands above the interlayered schists in outcrop, providing clean surfaces with little vegetation. While schists are interlayered throughout the lithology, the quartzofeldspathic gneiss is dominant in this unit. The EQG is highly recrystallised and affected by shearing, especially brittle deformation (Plate 2.a). Quartz and plagioclase layers are separated into small blocks by the action of brittle shear planes (Chapter 5.2.2, Minor-Scale Structures). These blocks contain a very weak biotite fabric. Chlorite and muscovite are manifest between these more competent blocks. They have a variable fabric depending upon the orientation of the blocks. Chlorite and muscovite however, are not intermixed within these areas. They remain separate entities, although they are aligned parallel to one another.

Plate 2

2.a Minor-scale brittle shearing in the Southern Quartzofeldspathic Gneiss unit. Unit is sheared dextrally.

2.b Protomylonitic ductile 'fins' of shearing which form 2m high outcrops of the Retrograde Schist unit. Outcrop displays dextral shearing.

2.c Minor-scale F_2 fold within the IPMS unit. Strong axial planar (S_2) fabric which is at a low angle to the layer parallel S_1 fabric. Within the fold hinge, the S_1 fabric is overprinted.

2.d Minor-scale F_3 fold within the Layered Gneiss unit.

2.e Minor-scale S-C fabrics within a protomylonitic shear band. Represent dextral shearing.

2.f Minor-scale S-C fabric orientations are influenced locally, especially by the presence of more competent structures. Asymmetry of pegmatitic boudin indicates dextral shearing.

2.g Minor-scale riedel and anti-riedel shear planes present in the same outcrop, and also the same layer of the Layered Gneiss unit. Consistent with dextral shearing.

2.h Minor-scale 'pop up' structure formed within the IPMS unit close to the shear zone.

* lens cap is 55mm in diameter

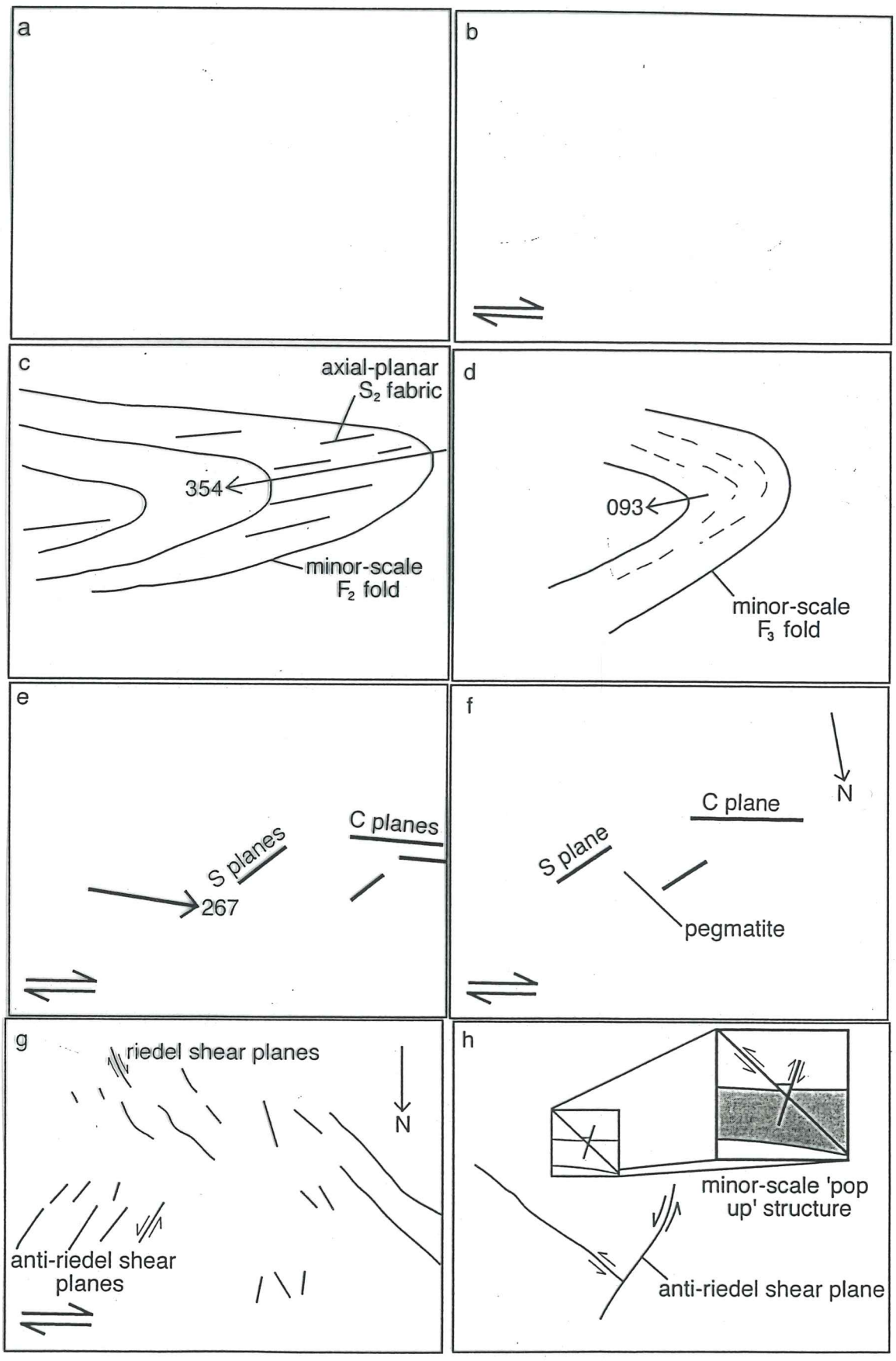
a
b
c
axial-planar
S_2 fabric
354
minor-scale
F_2 fold
d
093
minor-scale
F_3 fold
e
S planes
C planes
267
f
N
C plane
S plane
pegmatite
g
riedel shear planes
N
anti-riedel shear
planes
h
minor-scale 'pop
up' structure
anti-riedel shear plane

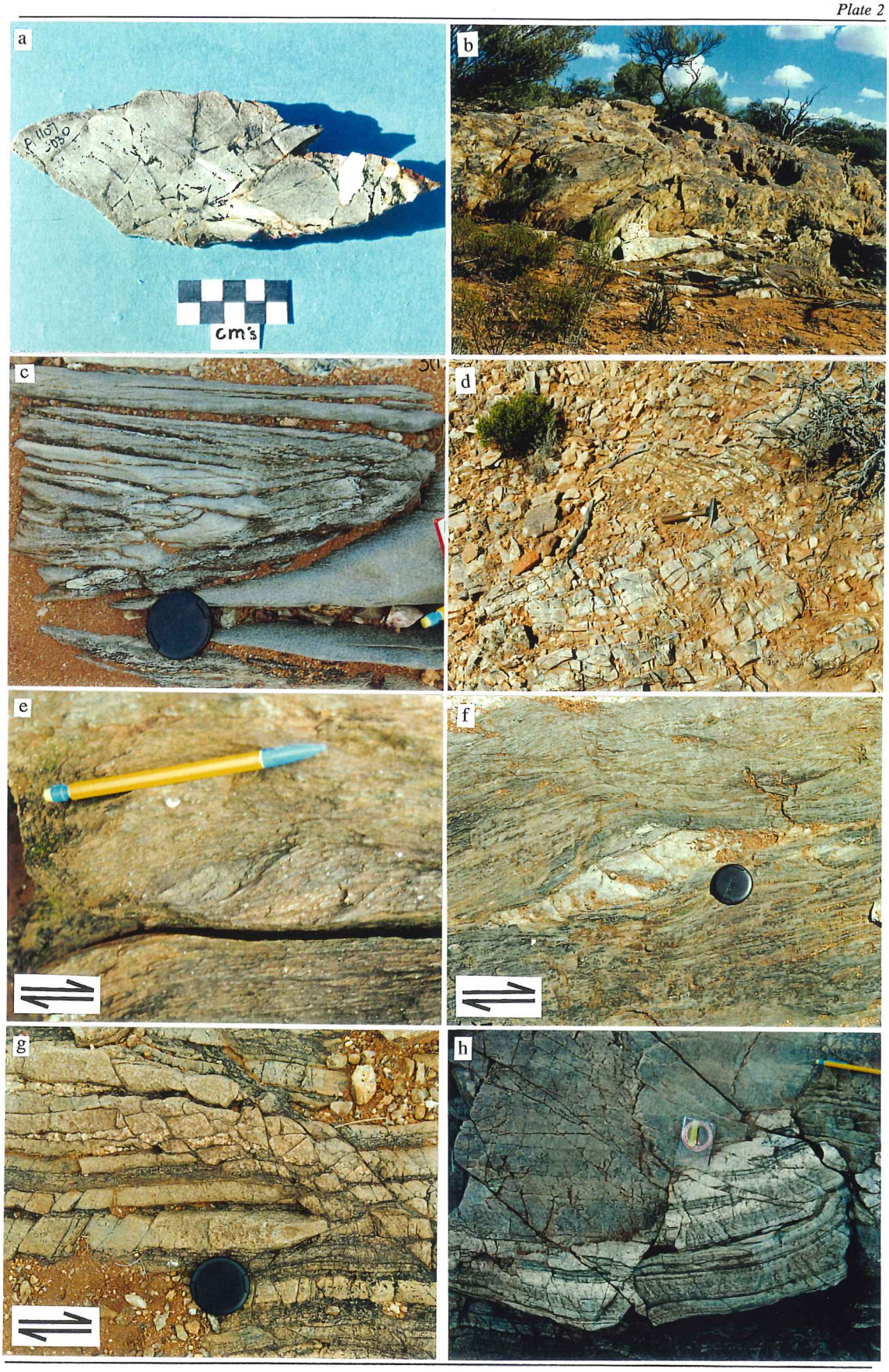
a
cm's
b
c
d
e
f
g
h

Retrograde schists (RS)

The RS unit represents the most intense areas of shear deformation and retrogression. They form ridges to the east of the shear zone and two metre high upstanding outcrops in many other parts (Plate 2.b). The RS lithologies are protomylonitic and have a strong chlorite fabric. Chlorite makes up more than 50% of the mineralogy, with 'augen-shaped' quartz aggregates between the fabric. This unit shows entirely ductile deformation and contains almost no biotite. Throughout most of the shear zone the RS unit represents thin (<2m wide) anastomosing shear bands, however at the eastern margin of the inlier it becomes as wide as 40m. This unit is similar to the characteristic unit of Olarian retrograde shear zones, which has been recognised by many previous authors within both the Olary and Broken Hill Domains (eg. Ashley *et al*., 1998).

CHAPTER 4 – Structural analysis of Gneiss Complex

4.1 Introduction

The Gneiss Complex, while less deformed than the Shear Zone lithologies, displays evidence of three major Olarian deformations. This chapter provides information on the fabric development and folding considered to be related to these deformations, along with associated metamorphic conditions. These characteristics of the GC are very important for comparison with structures within the SZ.

4.2 First Deformation (D_1)

S_1 is a layer parallel gneissosity and schistosity (Plate 1.e). The S_1 gneissosity is defined by 'P' (phyllosilicate-rich) and 'Q' (quartz-rich) zones, which form discrete boundaries between S_0 layers. S_1 generally strikes towards the NE, dipping steeply SE. Biotite and muscovite define the S_1 fabric most prominently. The more regionally developed S_1 fabric is the earliest formed within the mapping area; it is generally obliterated in more localised areas by overprinting S_2 and S_3 fabrics. The S_1 fabric is axial planar to isoclinal F_1 folds.

No F_1 fold hinges (see Forbes, 1991) are seen within the mapping area. A possible F_1 fold occurs in the northwestern schists and gneisses, where the repetition of an andalusite schist within stratigraphy may represent opposed limbs of a regional F_1 isoclinal fold (Figure 4.1). The fold closure does not outcrop as it is either sheared off to the west by the Walter-Outalpa shear zone, or hidden to the east beneath Adelaidean cover sequences. All younging indications on the eastern limb of the fold show NW younging overturned bedding, however it should be noted that no facing directions were found. The fold axial plane of such a structure would strike through the discontinuous calc-silicate unit.

The most prominent evidence for the metamorphic facies under which D_1 occurred is found within units to the NW of the mapping area. Andalusite porphyroblasts, which have the S_1 fabric wrapping around them, along with the presence of biotite, and amphibole, are indicative of amphibolite grade metamorphism.

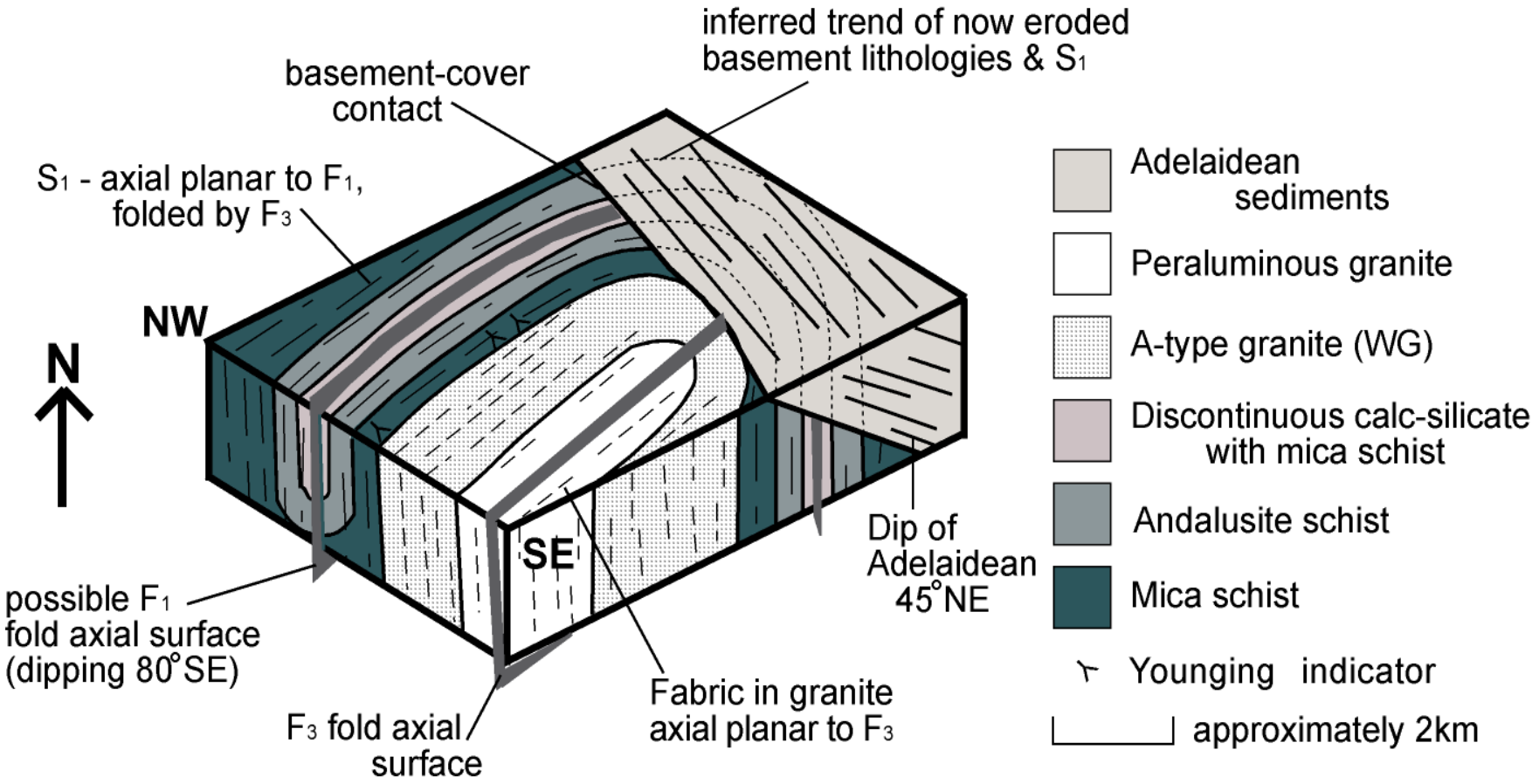

Figure 4.1 Schematic block diagram of a possible F_1 isoclinal synformal syncline refolded by an F_3 fold, north of the Walter-Outalpa shear zone, showing the refolding of the F_1 hingeline. Also represented is the unconformable contact between basement Willyama Supergroup lithologies and cover Adelaidean Supergroup lithologies. The F_3 fold axis plunges approximately 40° towards the NE.

4.3 Second Deformation (D_2)

The S_2 fabric is a well developed axial planar fabric seen only within local fold hinges that represent F_2 folds. Within these F_2 folds, the axial planar S_2 fabric (Plate 2.c) becomes dominant, overprinting and obliterating the S_1 fabric. S_0 remains visible, but is less obvious. The S_2 fabric is only recognisable within the NE portion of the mapping area and is best developed within pelite units where biotite defines the S_2 fabric (Plate 1.e).

Within the mapping area, F_2 folds are tight to open, Class 2 – similar style folds (Ramsay and Huber, 1987). All F_2 folds (Plate 2.c) contain a large component of hinge thickening and limb thinning. Minor F_2 folds contain a strong axial planar schistosity. F_2 fold axial planes generally trend N and dip steeply east. Some F_2 folds contain axial planes that dip less steeply and trend NE. Fold amplitude is quite variable, from 20cm to 5m.

The presence of a biotite foliation in the GC, representing the S_2 fabric, suggests that the retrogression of mineral assemblages had not begun during D_2. D_2 in the mapping area seems to have occurred under similar metamorphic conditions as D_1.

4.4 Third Deformation (D_3)

S_3 is represented by two discernible fabrics within the mapping area. Very localised crenulation of S_1 is one of these fabrics, which indicates that the development of S_3 is very lithologically dependent. The S_3 fabric is most strongly seen within schists, with the alignment of biotite, muscovite, and chlorite. While crenulations generally are gentle, with amplitude 40mm and height 25mm, some extremely localised S_3 crenulations possess amplitudes of only 3mm.

Within the granitic bodies north of the shear zone, a possible axial-planar fabric of a regional F_3 fold is present. This S_3 fabric is most prominently defined by biotite along with lesser amounts of magnetite, muscovite, and chlorite.

Minor-scale F_3 folds are found extensively throughout the mapping area, especially within layered and migmatitic gneisses. F_3 folds are class 1B – parallel folds (Ramsay and Huber, 1987). F_3 fold axial planes generally trend E, however this does vary with some trending in a more northeasterly direction. Folds classified as F_3 (Plate 2.d) are found up to 15m in amplitude and within the gneisses do not contain a penetrative axial planar fabric.

One major-scale F_3 fold axial plane trends towards the NE, within the Peraluminous granite (Figure 4.1). The effect of this folding is pronounced on lithologies north of the shear zone, showing folding of the units around an F_3 fold axis on magnetic imagery (Figure 1.2).

However Adelaidean sequences cover much of this. The presence of this fold on the southern side of the shear zone, where there is no Peraluminous granite representing the fold interior, is not confined. The granite fabric discussed earlier, is axial planar to this F_3 structure. However it is unclear if this is a true axial planar S_3 fabric, or part of the layer parallel S_1 fabric. Alluvium covers the fold hinge of the major-scale F_3 fold.

Folds generated by the shear zone formed later than F_3 folds, however Ashley *et al.* (1997) documents shear zone structures as representing a continuation of D_3 deformation. Shear folds are discussed in Chapter 5.2.2 as part of the Minor-Scale Structures of the shear zone.

F_3 folding events affect earlier folding, resulting in Type 2 – luniform interference patterns (Ramsay and Huber, 1987), as seen in Figure 4.2. The migmatitic gneiss south of the shear zone shows folding most prominently. This lithology shows luniform shapes on a minor-scale. Figure 4.1, a schematic interpretation of the lithologies north of the shear zone, shows the formation of a partial luniform shape.

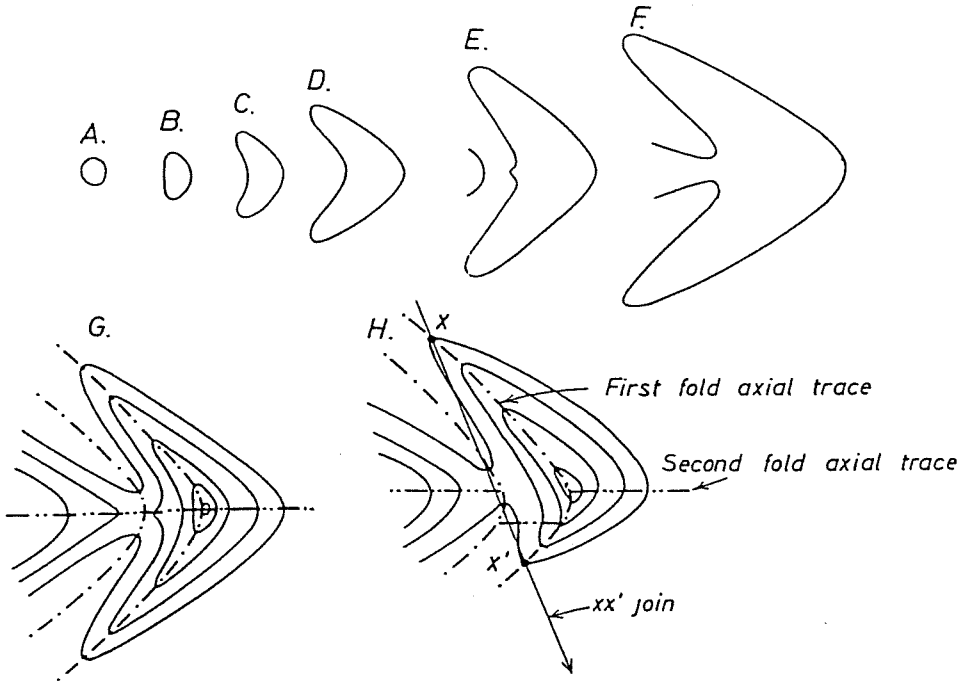

Figure 4.2 Luniform interference patterns (from Ramsay and Huber, 1987).

4.5 Fourth Deformation (D_4)

An S_4 fabric, reported to be formed late D_3 (Ashley *et al*., 1997), is confined to the shear zone. However, Sm-Nd dating of minerals forming this fabric, show a Delamerian deformation age – see Chapter 5.4, Sm-Nd Dating of the Shear Zone. It should be noted that the shear zone is interpreted to have initiated prior to the Delamerian deformation, however there is strong Delamerian overprint. Timing of shear zone initiation is discussed in Chapter 5.

The S_4 schistosity is the shear zone fabric and therefore it is defined by the alignment of the retrograde minerals, especially chlorite, sericite, and elongate aggregates of quartz. Chlorite forms the dominant schistosity, replacing biotite. S_4 has a relatively variable trend as it follows an anastomosing pattern of shearing. It generally strikes between E-W to SE-NW. As the S_1 fabric approaches the shear zone, it rotates into parallelism with the S_4 fabric. This S_4 fabric dips steeply towards the south.

Near the outer boundaries of the shear zone, magnetite and biotite increasingly form the fabric, although some magnetite probably arose through reactivation of the shear zone (Chapter 5.2.3 Microstructures). The shear zone defines the latest fabric to form as it transects all other structures in the basement lithologies, including F_2 (and therefore S_2) and F_3 folds.

The presence of low-grade metamorphic mineral assemblages, particularly muscovite and chlorite, characterise this deformation. Sericite replacement of some former andalusite porphyroblasts within the GC further indicates a retrogressive deformation event under greenschist metamorphic conditions.

4.6 Discussion

This study supports the interpretation of three Olarian deformation events, as was first recorded by Berry *et al*. (1978). However some differences have arisen within the mapping area.

The inferred major F_1 isoclinal fold within the NE of the mapping area represents a transport direction towards the NW. This opposes the early studies, which infer a transport direction towards the SE. However some of the previous work correlates the deformation history of the OD directly with that of the BHD. This may not be entirely the case as

unpublished work is finding increasing evidence to support a northern direction of transport during D_1 (Paul pers comm., 1998).

D_2 and D_3 have been interpreted as separate deformational events; F_2 folds trend N to NE and contain a strong axial planar schistosity, while F_3 folds trend E to NE and do not contain any visible axial planar fabric.

Some authors have indicated that retrograde metamorphism began during OD_2 (eg. Clarke *et al*., 1986). Mineral assemblages within the mapping area have not supported this. There is no conclusive evidence that retrograde metamorphic conditions prevailed during OD_2, however this deformation does represent a stabilisation of earlier prograde metamorphic conditions.

The retrograde shear zone, while showing a strong Delamerian overprint of structures and fabrics, must have initiated pre-Delamerian. Deformation mineral assemblages within the shear zone however, have completely recrystallised during Delamerian reactivation of the shear zone.

CHAPTER 5 – Walter-Outalpa Shear Zone

5.1 Introduction

The NW trending Walter-Outalpa shear zone is the most prominent feature of the eastern Weekeroo inlier. It is at least 10km long and up to 40m wide. To date, its geometry and kinematics have not been documented, as is the situation with all shear zones within the OD. This chapter provides geometric and kinematic information on the shear zone (Figure 3.1) and its features. Although named the 'Walter-Outalpa Fault' on many geological maps, it is in fact a major shear zone, as displacement is achieved over a zone containing numerous smaller displacements.

The shear zone has been studied at three observational scales. A major-scale interpretation, describes structures exceeding 20m or the outcrop scale, a minor-scale interpretation, studies visible structures at the outcrop and hand specimen scale, and a microscopic study shows structures not able to be studied with the naked eye.

The Walter-Outalpa shear zone is mapped (Figure 3.1) to include prominent shear bands, which are represented by protomylonitic ductile shear fabrics. These bands (usually 2m wide) anastomose between less deformed blocks (up to 200m wide) which display predominantly brittle structures on a minor-scale.

5.2 Structural Interpretation

5.2.1 Major-Scale Structures

The most dominant feature of the Walter-Outalpa shear zone is that it transects all other basement lithologies and structures. This includes all Willyama Supergroup metasediments and the granitoids. This crosscutting relationship is seen prominently on magnetic imagery (Figure 1.2) with the shear zone represented by a linear magnetic low.

Along much of the shear zone, where there is predominantly ductile-brittle shearing, the topography is low and the shear zone is defined by creek lines or lower lying areas. At the eastern end of the shear zone, a zone of ductile shearing dominates, and mylonitic 'fins' (Plate 2.b) define an upright ridge. Along the shear zone, outcrops of these 2m high ridges stand above surrounding lithologies, and are more resistant to the effects of weathering and erosion. This is also seen in the west where two thin bands (5m wide) trend parallel to one another in a SE-NW orientation. The southern shear band becomes highly mylonitic and defines the beginnings of low hills, whereas the northern shear band trends predominantly along a creek bed (Figure 3.1).

Figure 5.1 Subareas showing rotation of fabrics from the Gneiss Complex into parallelism with the Walter-Outalpa shear zone. Contoured data of poles to planes are plotted.

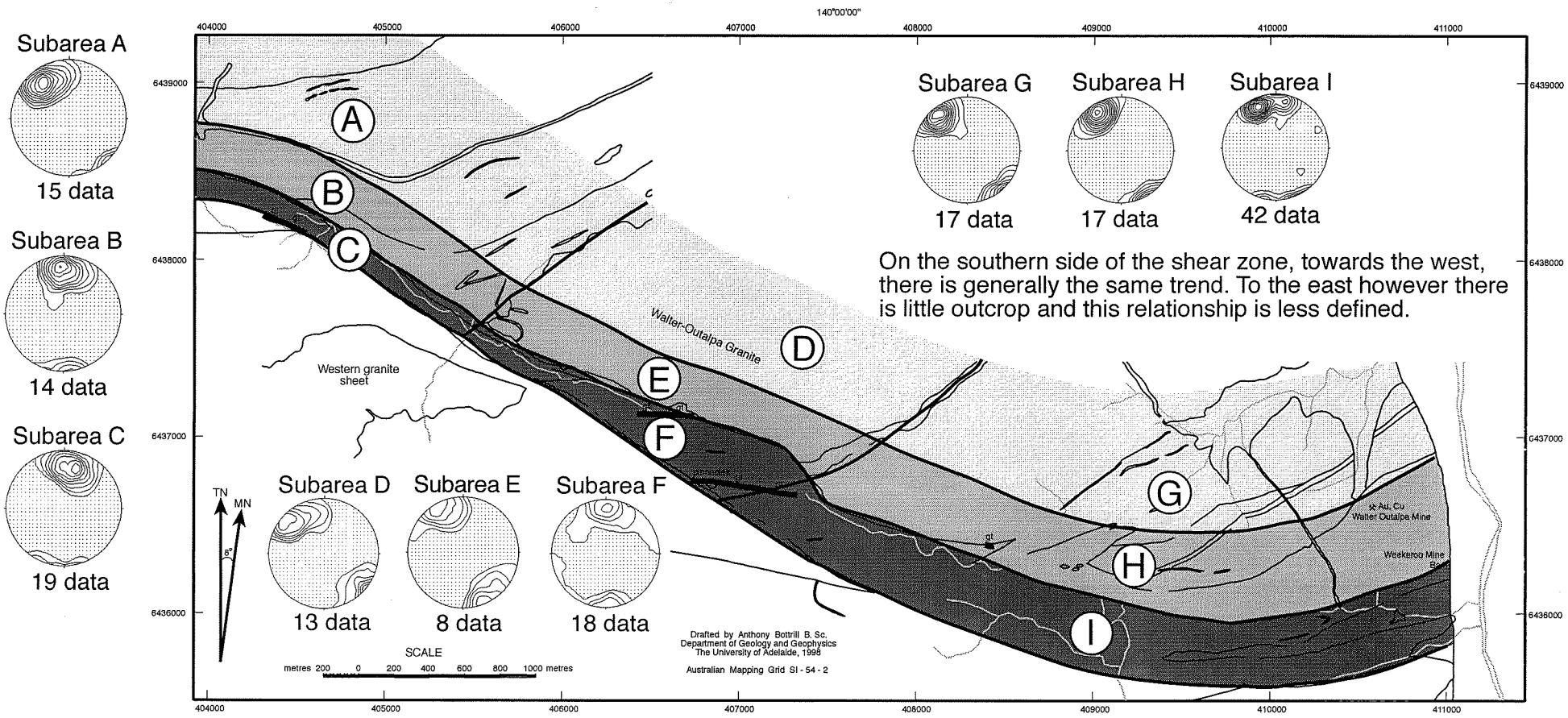

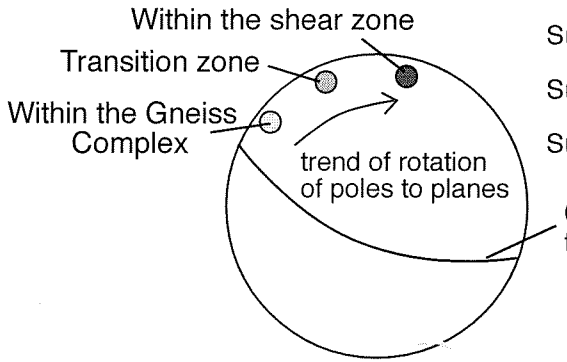

Subareas A, D, and G - fabrics within the Gneiss Complex.

Subareas B, E, and H - fabrics within the transitional zone between the shear zone and the Gneiss Complex.

Subareas C, F, and I - fabrics within theWalter-Outalpa shear zone.

The orientation of the two shear bands, compared to other shear bands, and the overall shear zone, indicates that the two bands represent the C planes of a large scale S-C fabric (Figure 3.1). S planes represent anastomosing metre wide bands, which adjoin these two main shear bands. Gneissosity within the layered gneiss strikes parallel to these S shear bands, which trend at approximately 35° to the C shear bands. S shear bands generally strike E-W. Large scale S-C fabric analysis indicates a dextral sense of shearing.

The relatively less deformed blocks, between anastomosing shear bands, preserve Olarian deformations and brittle shearing, on a minor-scale. These blocks are most prevalent within the Layered Gneiss unit, and may be up to 200m in length.

Close to the Walter-Outalpa shear zone, lithological boundaries and their S_1 fabric rotate into parallelism with the shear fabric. This rotation indicates a dextral shear sense (Figure 5.1). The subareas within Figure 5.1 show this rotation of lithological fabrics from the GC, through a transition area, into the shear zone. The orientation of splaying shear bands from the main shear zone also indicates dextral shearing.

The most important feature of the shear zone, is the occurrence of a purely ductile shear fabric at the eastern end of the shear zone. This fabric extends for 1500m towards the west from the basement-cover contact. Small outcrops of this are found throughout the shear zone. This protomylonitic ductile shear fabric is distinguished from the main shear fabric in which ductile-brittle conditions prevail. Protomylonitic ductile fabrics within the shear zone are generally less than three metres thick. This ductile fabric however, represents a thickness of approximately 40m. The mineralogy of this fabric also shows almost complete retrogression (see Chapter 5.2.3 Microstructures). The eastern ductile shear zone may represent the earliest formed shear zone, as it represents a true ‘retrograde schist zone’ (discussed in Chapter 5.3, Comparison with other Shear Zones).

Within the centre of the mapped area, the shear zone and lithological boundaries are offset over a distance of 200m (Figure 3.1). This shearing extends into the WG towards the NW. This shear orientation, at a low angle to the shear zone, dextrally displaces the Walter-Outalpa shear zone and lithologies. This movement is synthetic to that of the overall shear zone, therefore it may represent a major-scale riedel shear plane. Figure 5.2 represents two possible models for the development of such a feature.

Splaying of shear bands, on the northern side, towards the eastern end has sheared two large-scale wedges (up to 200 wide) of layered gneiss into peraluminous granite (Figure 3.1). This is a typical occurrence towards the east where the shear zone splays towards the NE.

5.2.2 Minor-Scale Structures

5.2.2 a) *S-C Fabrics*

S-C fabrics are observed on all three scales of the Walter-Outalpa shear zone. Blenkinsop and Treloar (1995) divided the two planar fabrics, which are found characteristically in shear zones, into a sigmoidal penetrative foliation often referred to as the S foliation, and discrete planar shears that displace the foliation. These shear planes represent slip surfaces known as C surfaces (Berthé *et al*., 1979). C surfaces are defined as being parallel to the local shear plane (Blenkinsop and Treloar, 1995). S-C fabrics present a reliable kinematic indicator, especially within the Walter-Outalpa shear zone.

S-C fabrics within the Walter-Outalpa shear zone (Plate 2.e) almost exclusively show a dextral sense of shear. This is indicated by clockwise rotation of C planes to encounter the strike of the S plane (Behrmann, 1987). Minor-scale S-C fabrics are most prominent within the retrograde schist material, representing a protomylonitic lithology.

Of interest are variations in the orientation of S and C planes along the length of the shear zone. This variation is with respect to each other, and with respect to the overall orientation of the shear plane.

For a detailed analysis of the shear zone, it has been divided into five main subareas (Figure 5.3). Rose diagrams have been plotted for both S planes and C planes, with the α angle (Blenkinsop and Treloar, 1995) between the C and S planes measured.

Of most importance is the orientation of the C plane, as this theoretically approximates the local bulk shear plane. *Subarea 1* has three well defined orientations for the C plane. These are strongly influenced by the three most prominent shear zone outcrops in the subarea. The orientation of these C planes is generally NW-SE dipping 70° south. The two more easterly C plane orientations are approximately equal to the orientation of the average bulk shear plane (an average of C plane orientations along the shear zone). The orientation of the bulk shear plane approximately strikes 112°. S planes are quite variable, although their envelope range is similar to that of the C planes. They commonly lie at an α angle of 32° to the C plane. This is the closest average angle seen between C and S planes.

C planes for *subarea 2* have a smaller range and overall more closely approximate the orientation of the shear zone than *subarea 1*. S planes average an α angle of approximately 34° to the C planes and trend ENE.

C planes within *subarea 3* are highly variable, and strongly related to individual outcrops. They vary between outcrops and show six discrete orientations. This subarea represents a perturbation of the shear orientation due to a major-scale offset of the Walter-

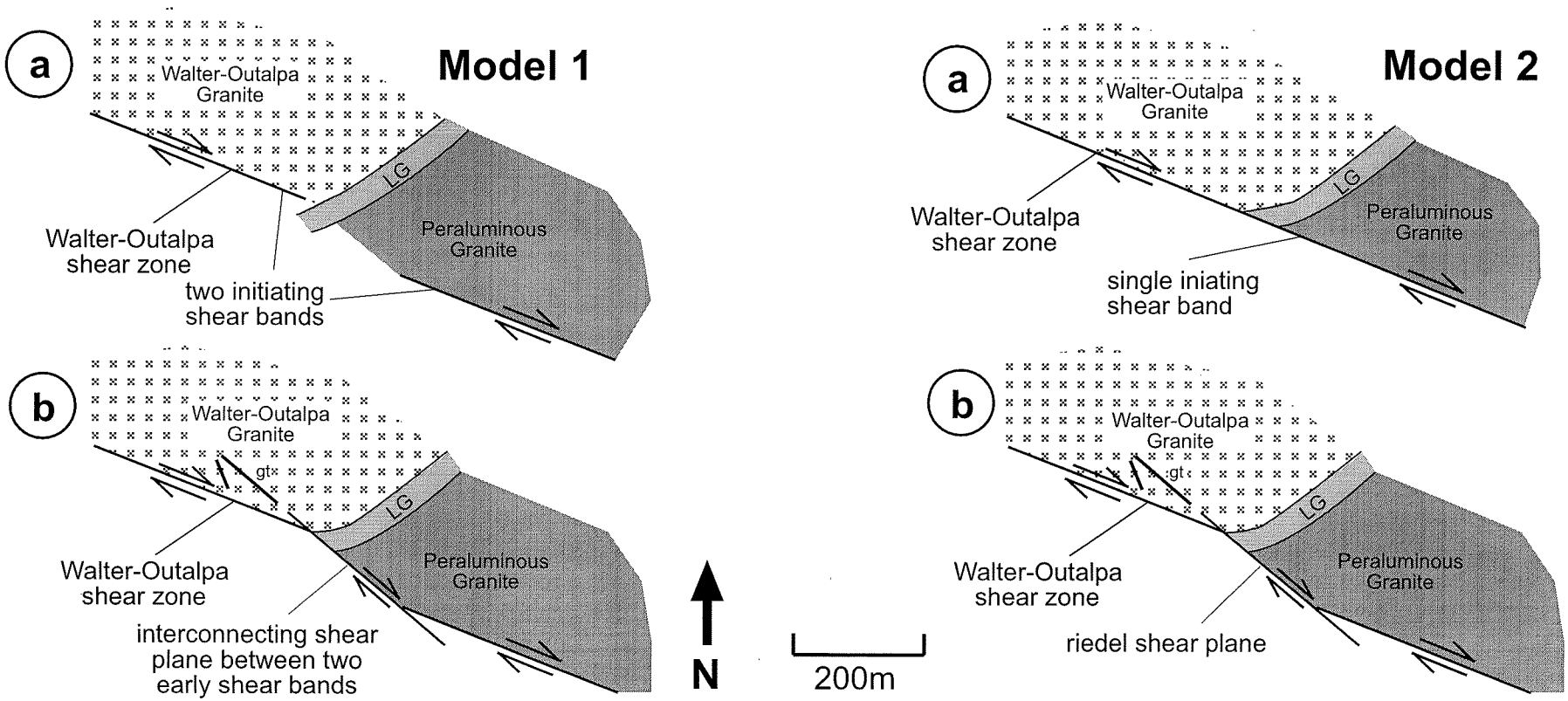

Figure 5.2 Two schematic models to account for low angle synthetic offset development within the Walter-Outalpa shear zone on a major-scale. Model 1 interprets that the low angle shear plane is an interconnecting shear band between two initiating shear bands. This comes from the interpretation of Wilcox *et al.* (1970) that main through going shear zones are only a late stage development, through an interconnecting series of early fractures. Model 2 interprets that the low angle shear plane is a major-scale riedel shear plane that offsets the shear zone. Model 2 would represent a displacement of approximately 200m, while Model 1 would cause relatively small displacement of local lithologies. The end products of the models both account for the shear zone as it is visible now.

Outalpa shear zone. The dominant C plane strikes NW-SE, 25° from the overall shear zone orientation. Through this zone, C planes align more closely with the overall orientation for riedel shear planes (towards 134°). The α angle between the planes is larger through this region, 42°.

C planes within *subarea 4* most closely approximate the average true shear plane. The range of C plane orientations includes the overall shear zone orientation, and generally strikes ESE. This relates effectively to only two outcrops providing measurable S-C fabrics. S planes strike towards 070° and keep a consistent α angle of 40°.

Subarea 5 contains the most variable S-C orientations. Within this subarea the shear zone splays towards the NE, which is seen in the trend of C planes (Figure 3.1). C planes rotate from trending SE to almost NE due to the measurement of C planes on splaying shear bands. S planes are also highly variable, and is strongly dependent on individual outcrops. While the α angle between S and C planes averages 36°, the angle is highly variable. It has been measured at up to 60° and as low as 19°.

In general, the orientation of S-C fabrics is variable along the Walter-Outalpa shear zone, and is strongly influenced by local conditions within individual outcrops (Plate 2.f). The highly ductile nature of the fabric results in S-C planes representing only the local strain field. Averages of this over the whole shear zone give a genuine representation of the true shear plane orientation. The average α angle between S and C planes is approximately 36°. This is consistent with angles measured by Blenkinsop and Treloar (1995) when measuring α angles of S-C fabrics within medium grained shear zone lithologies (finer grained lithologies tend to contain α angles with a tighter angle, 10°-30°). The most important information gained from S-C fabrics is a consistent dextral sense of shear.

5.2.2 b) *Synthetic and Antithetic Brittle Shear Fractures*

The formation of brittle shear fractures at an angle to the bulk shear plane orientation is seen in numerous outcrops along the length of the Walter-Outalpa shear zone. These are most prominently represented within the quartzofeldspathic and layered gneisses. These planes display a brittle phase of shearing, which show centimetre-scale subhorizontal displacement of competent quartz-rich layers. This displacement becomes ductile within the mica-rich interlayers, where it rotates towards parallelism with C planes.

Low angle brittle shear planes, representing synthetic movement to that of the overall shear zone, are called riedel (R_1) shear planes (Tchalenko, 1970; McClay, 1987). They are the most numerous type of brittle shear planes found and consistently show a NW-SE orientation (Figure 5.4). At the outcrop scale, riedel planes lie parallel to one another and are

Figure 5.3 Variation of S and C fabric orientations displayed on rose diagrams for five main subareas within the Walter-Outalpa shear zone. Rose diagrams - Interval: variable; Radius: 20 uniform.

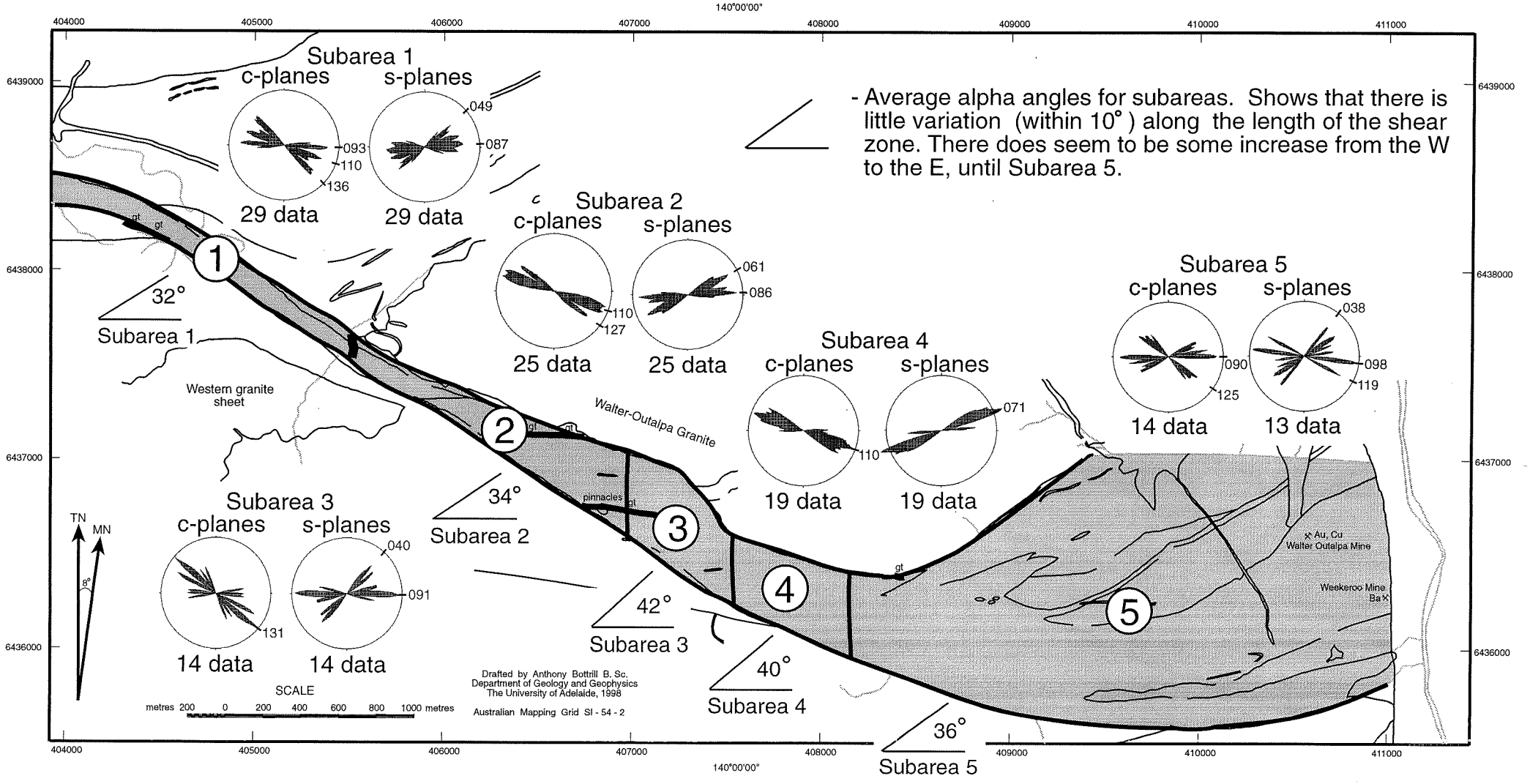

Figure 5.4 Variation of riedel and anti-riedel shear plane orientations displayed on rose diagrams for shear zone subareas C, F, and I. Rose diagrams - Interval: variable; Radius: 20 uniform.

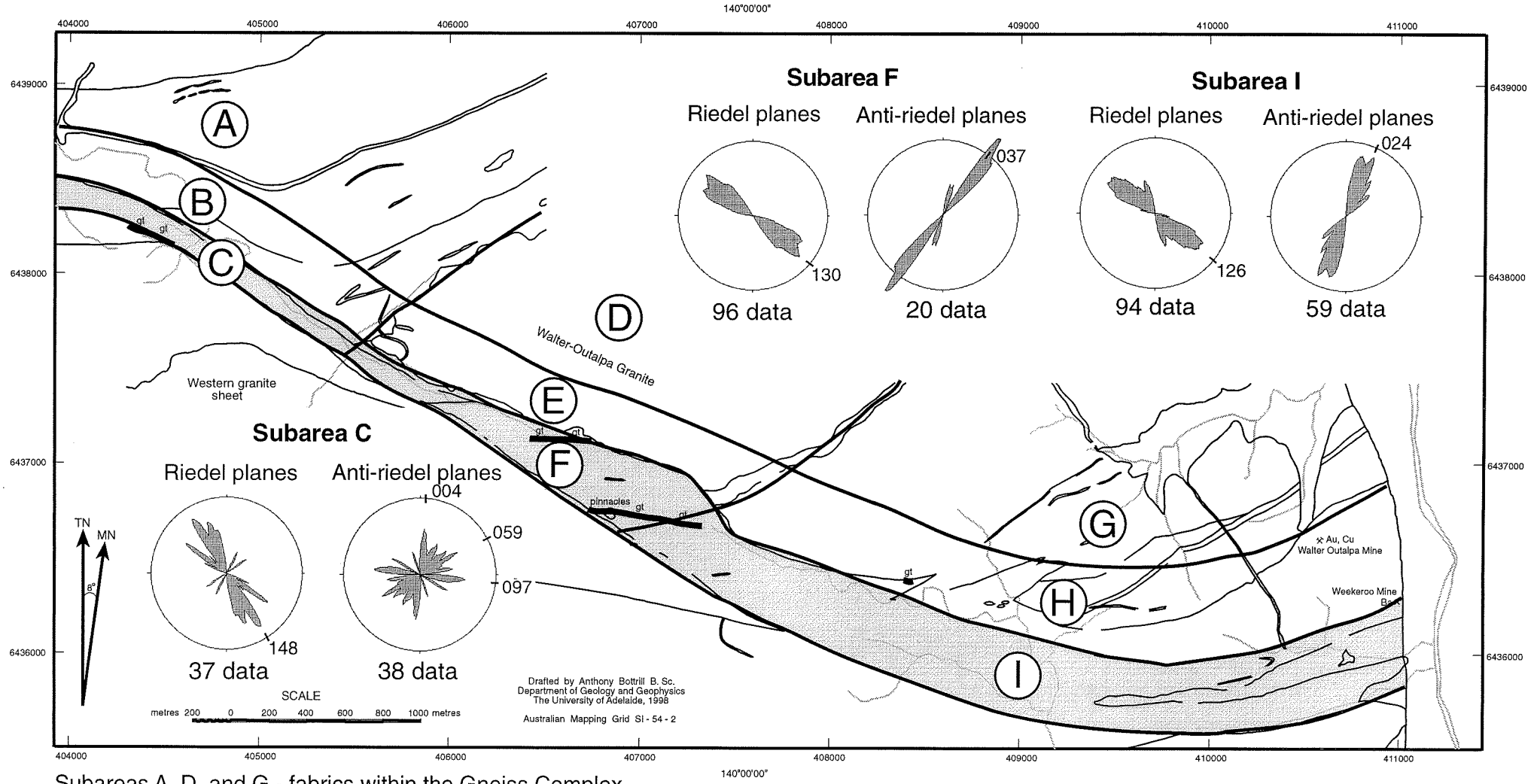

Subareas A, D, and G - fabrics within the Gneiss Complex.

Subareas B, E, and H - fabrics within the transitional zone between the shear zone and the Gneiss Complex.

Subareas C, F, and I - fabrics within the Walter-Outalpa shear zone.

spaced approximately 30mm apart. Some planes may show rotation near ductile mica-rich layers.

Within the layered gneiss, individual riedel shear planes may be traced through the mica-rich layers into an adjacent quartz-rich layer (Figure 5.5). Through the mica-rich layers, the shear plane will align with the foliation before rotating back into alignment with the next brittle riedel plane of a quartz-rich layer. Between adjacent outcrops, the orientation of riedel shear plane sets may vary slightly. These variations represent minor changes in the orientation of the shear strain and its intensity. However orientations tend to remain within a 45° envelope centred around 134° (Figure 5.4). Riedel shear planes dip relatively steeply, averaging 65° S.

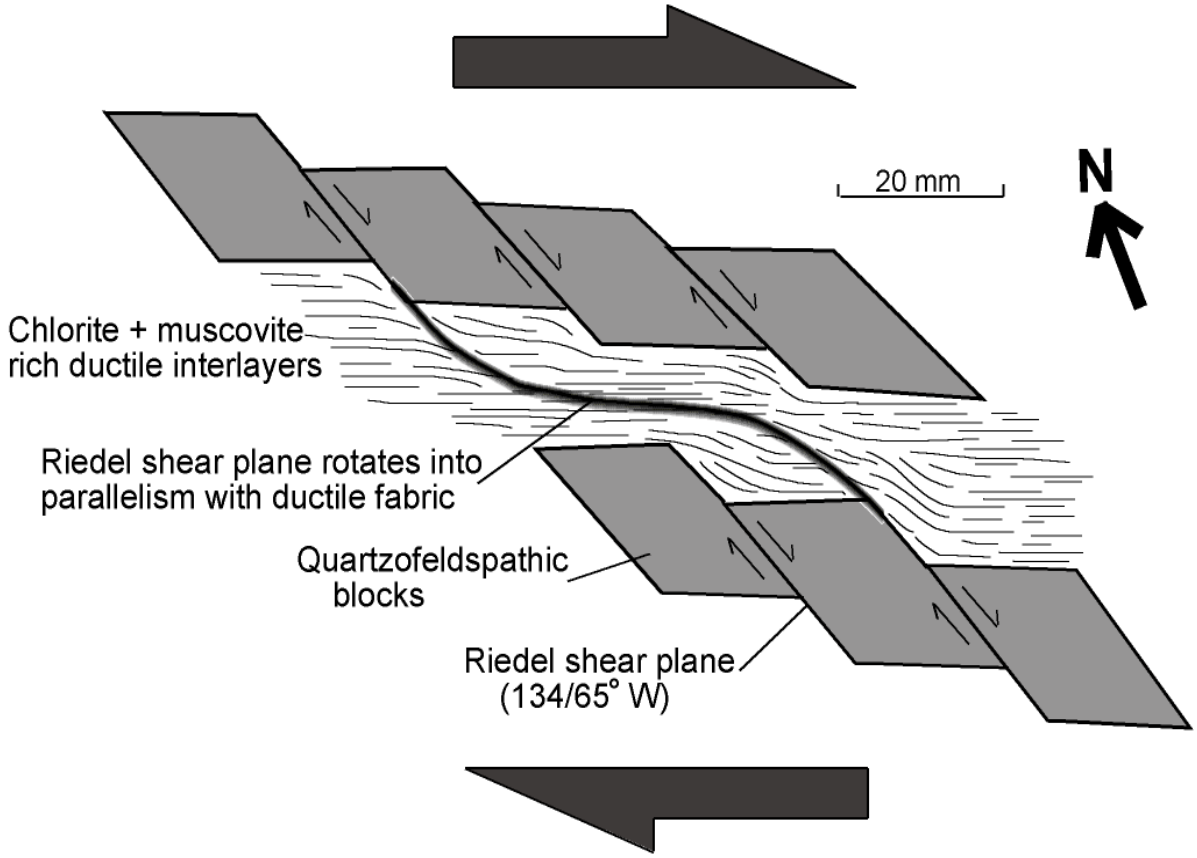

Figure 5.5 Brittle riedel shear plane, within quartzofeldspathic layer, rotates into parallelism with ductile fabric within the chlorite + muscovite rich schistose interlayers.

Figure 5.4 shows the variations in orientation of riedel shear planes within the shear zone. There is division of the shear zone into separate subareas, from *subarea A* to *subarea I*. Shear planes were only measured in *subareas C*, *F*, and *I*, which represent shear zone subareas. From this figure, the consistency of the riedel plane orientations is evident.

An example of riedel shear planes showing true displacements, rather than offset, is shown in Figure 5.6. Four riedel shear planes transect the fold axis of a minor isoclinal fold, and act as a generation line for piercing points, therefore revealing true displacement.

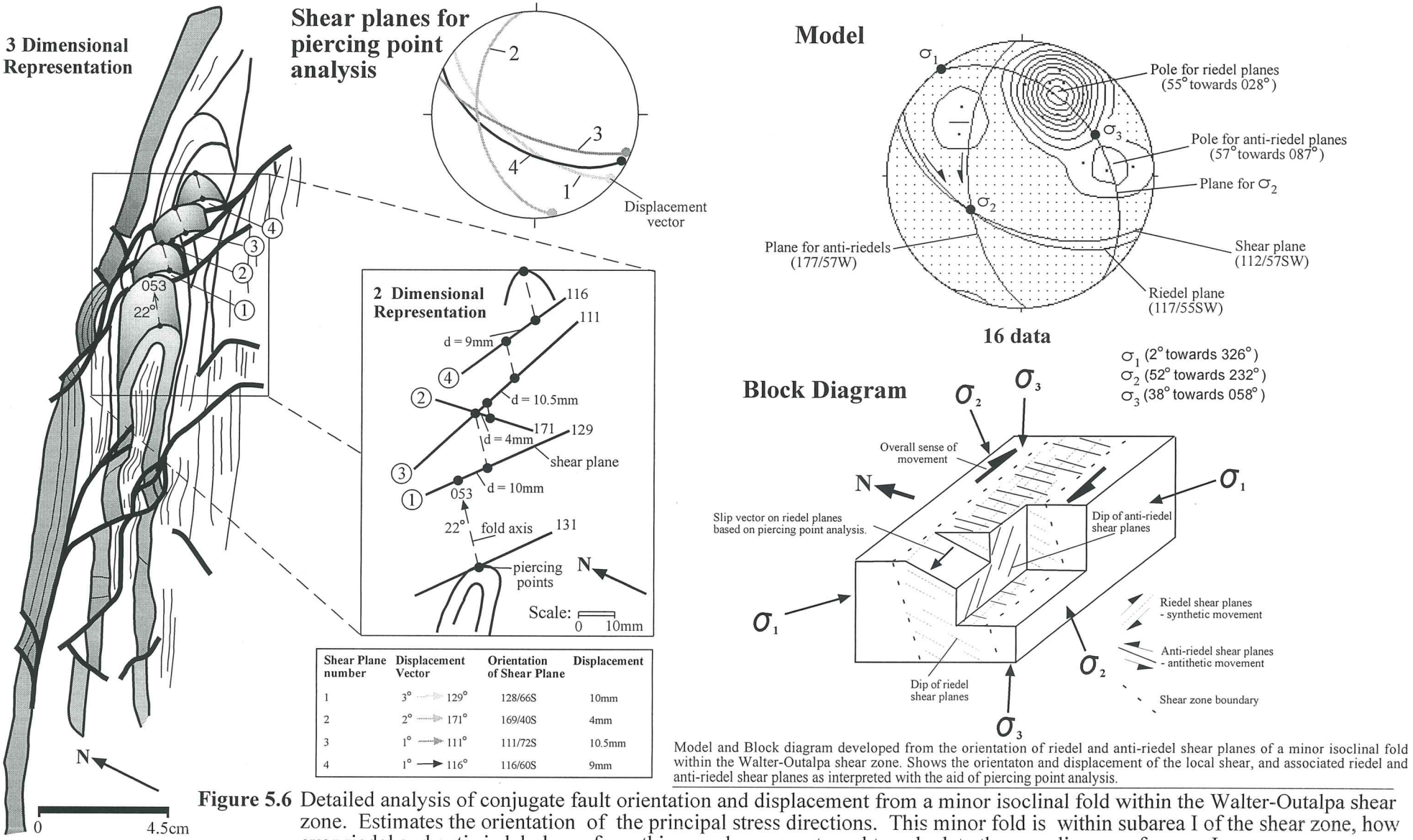

Shear Plane number	Displacement Vector	Orientation of Shear Plane	Displacement
1	3° → 129°	128/66S	10mm
2	2° → 171°	169/40S	4mm
3	1° → 111°	111/72S	10.5mm
4	1° → 116°	116/60S	9mm

Model and Block diagram developed from the orientation of riedel and anti-riedel shear planes of a minor isoclinal fold within the Walter-Outalpa shear zone. Shows the orientaton and displacement of the local shear, and associated riedel and anti-riedel shear planes as interpreted with the aid of piercing point analysis.

Figure 5.6 Detailed analysis of conjugate fault orientation and displacement from a minor isoclinal fold within the Walter-Outalpa shear zone. Estimates the orientation of the principal stress directions. This minor fold is within subarea I of the shear zone, how ever riedel and anti-riedel planes from this sample were not used to calculate the rose diagrams for area I.

Displacements are small; representing approximately 10mm, for riedel planes spaced 10mm apart.

Anti-riedel (r´) shear planes form a conjugate set to riedel shear planes (Tchalenko, 1970; McClay, 1987). These planes exhibit an antithetic sense of movement to that of the overall shear zone. Anti-riedel planes lie at a high angle to the shear zone orientation, and are most frequently represented within the shear zone as bookshelf structures. As with riedel shear planes, some anti-riedel shear planes may show slight rotation near ductile mica-rich layers. Dip on anti-riedel shear planes is very similar to that of riedel shear planes, averaging 60° W. Offset along anti-riedel shear planes in the Walter-Outalpa shear zone is sinistral.

Orientation of these planes is more variable than those of the riedel shear planes (Figure 5.4). Within *subarea C*, the orientation of anti-riedel planes is highly variable. This represents variations between anti-riedel shear planes of different outcrops. The variation between planes in this subarea is up to 90°. Anti-riedel shear may vary between N-S and E-W. Within *subareas F*, and *I*, the orientation of anti-riedel planes has a greater consistency (Figure 5.4). Within *subarea F*, the orientation of these shear planes is towards 035°, and they lie perpendicular to associated riedel planes. *Subarea I* has an orientation striking towards 015°, and a tighter angle to its associated riedel planes - approximately 75°.

Angles between riedel and anti-riedel planes are always greater than 45°, however these planes are most prominently at high angles, between 70-90°.

Both riedel and anti-riedel shear planes may be seen in the same outcrop (Plate 2.g), even along the same layer. In general, however, riedel shear planes are the dominant brittle shear plane formed. Horizontal offsets achieved are usually greater along riedel shear planes.

One outcrop showed the formation of these conjugate planes, resulting in small scale ‘pop up’ structures (Plate 2.h).

5.2.2 c) *Folding*

Folding caused by shearing within the Walter-Outalpa shear zone occurred after the OF_3 folding event (as shear zone structures overprint all other folding). The asymmetrical orientation of the shear folds consistently indicates dextral shearing (Plate 3.a, 3.b). The short limb of shear folds in the shear zone is always the western limb. This indicates that the folds are sheared dextrally towards the west. Recognisable folds are most prominently formed in the layered gneiss. The trend of the fold axial plane is always towards 250°-070°. Fold types are variable, however shear folds often display limb thinning on the shortened limb. Further shearing of these folds would result in the shortened limb being entirely sheared out. The strain ellipse for the shear zone (Figure 5.7) shows the orientation of the

Plate 3

3.a Minor-scale asymmetric shear fold in a quartz vein. Minor-scale S-C fabrics are also prevalent and both represent dextral shearing.

3.b Minor-scale asymmetric shear fold within a quartzofeldspathic layer. Asymmetry of fold consistent with dextral shearing.

3.c Minor-scale F_3 fold transected by an apparent minor-scale reverse fault. Thrust plane parallel to bedding planes on the western limb of the fold (to the right of the photo).

3.d Slickenside lineations formed on a quartz vein. Indicate the displacement orientation. 'Step' analysis of slickensides, along with dextral shear indicators, interpret the displacement direction to be up plunge.

3.e Rotated garnet porphyroblast containing a chlorite and muscovite pressure shadow, within the Garnet-chlorite Schist unit. Consistent with dextral shearing.

3.f Chlorite and muscovite pressure shadow of a magnetite porphyroblast, within the Garnet-chlorite Schist unit. Represents dextral shearing.

3.g Microscopic S-C fabric preserved by chlorite and muscovite within the Garnet-chlorite Schist unit. Indicates dextral shearing.

3.h Elongate aggregates of recrystallised quartz minerals defining the S_4 fabric along with chlorite and muscovite within the Retrograde Schist unit.

* lens cap is 55mm in diameter; 'Max' is 30mm in width.

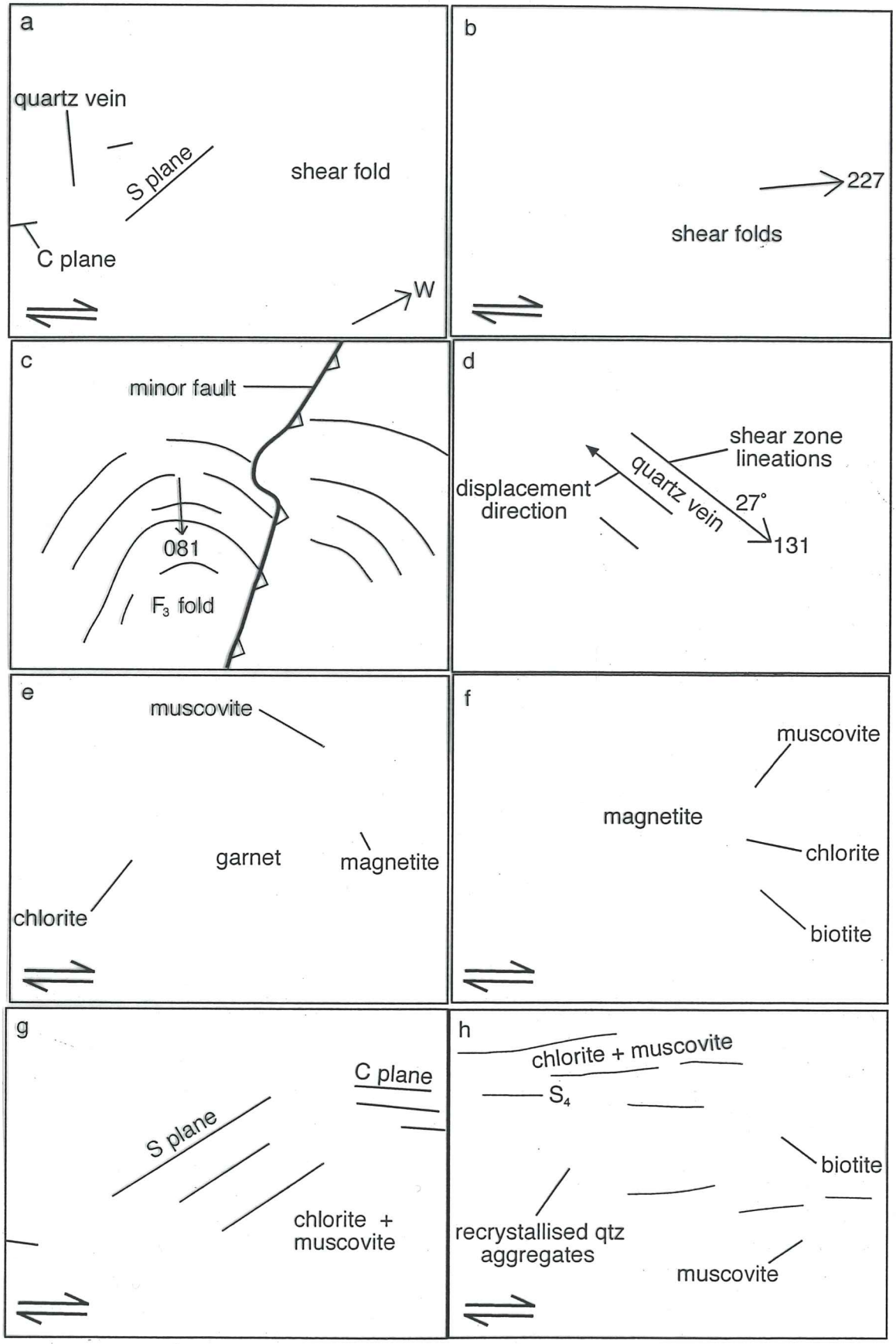
a
quartz vein
S plane
shear fold
C plane
W
b
227
shear folds
c
minor fault
081
F_3 fold
d
shear zone lineations
displacement direction
quartz vein
27°
131
e
muscovite
garnet
magnetite
chlorite
f
muscovite
magnetite
chlorite
biotite
g
C plane
S plane
chlorite + muscovite
h
chlorite + muscovite
S_4
biotite
recrystallised qtz aggregates
muscovite

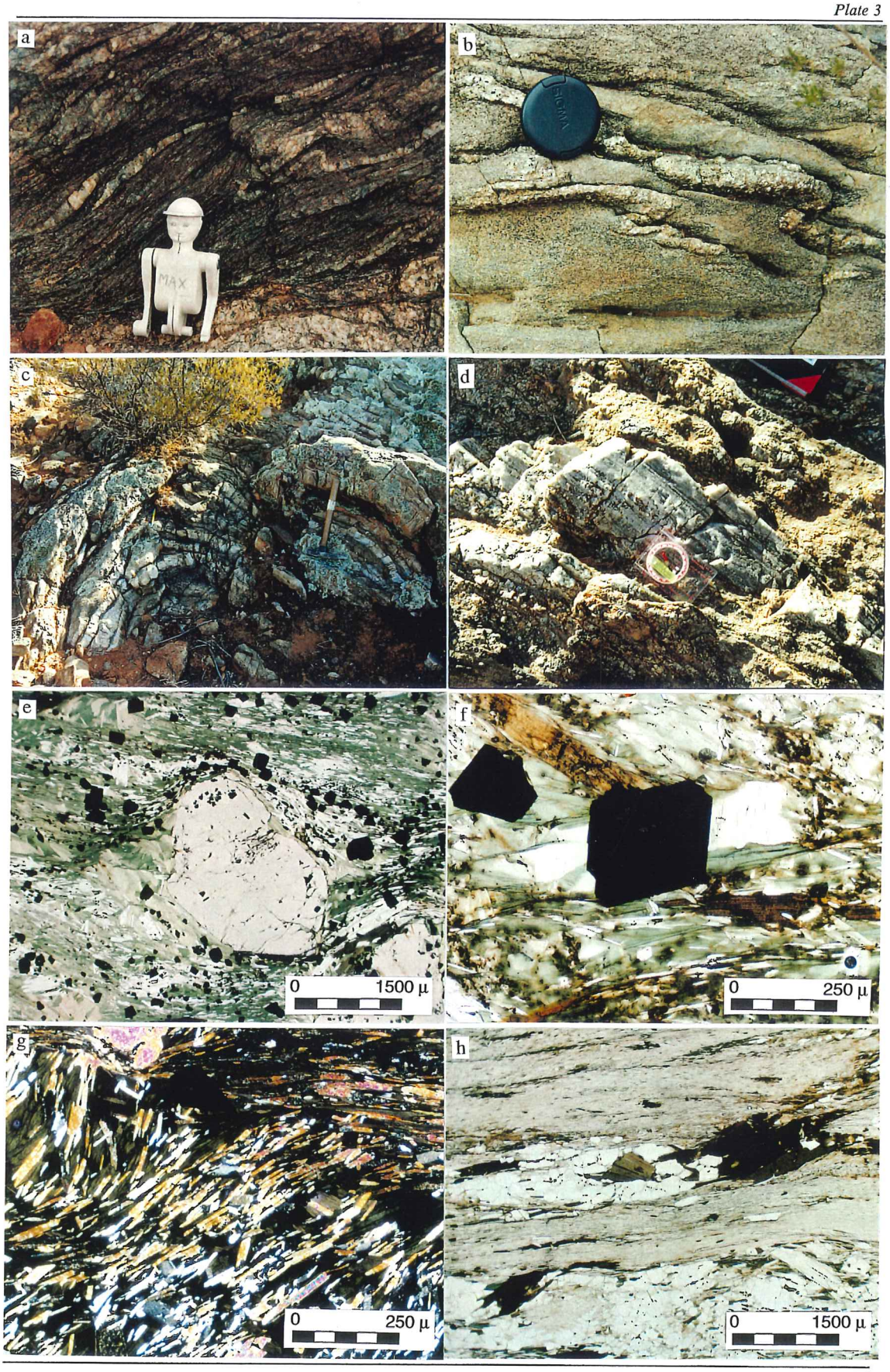
a
MAX
b
SIGMA
c
d
e
0 1500 µ
f
0 250 µ
g
0 250 µ
h
0 1500 µ

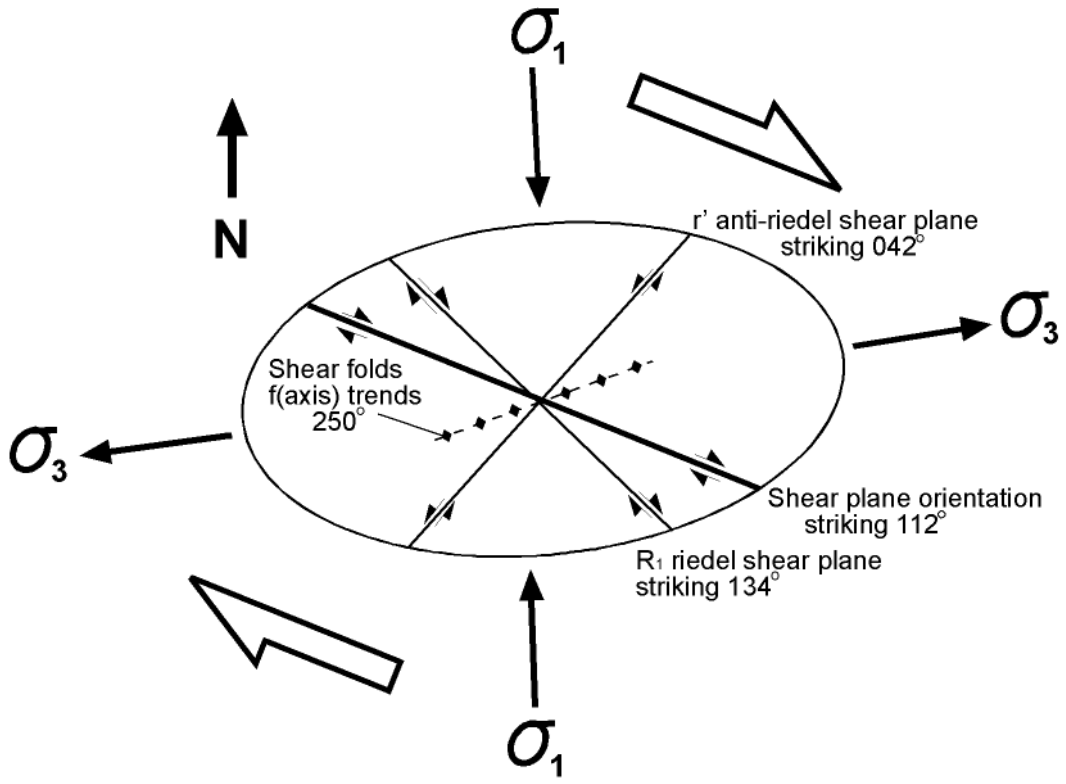

Figure 5.7 Strain ellipse associated with the Walter-Outalpa shear zone. Orientations taken from field measurements. Based on figures from Biddle and Christie-Blick (1985), and McClay (1987).

shear fold axial plane towards 250°, however this is at a relatively high angle to the orientation of the shear zone. A possible explanation for this feature is that the shear folds formed from a continuation of the folding of earlier developed folds. Therefore the shear folds would have started forming at a higher angle to the shear plane, resulting in the end product of the folds being at a higher orientation to the shear plane than expected. It is unclear as to the effect of folding on displacement along the shear zone. Only small examples (<150cm amplitude) of shear folds are present.

5.2.2 d) *Faulting*

Larger scale faulting within the shear zone is relatively rare. An amphibolite dyke is faulted within the creek on the western boundary of the main body of the Walter-Outalpa Granite (Figure 5.8). This displacement represents dextral faulting along parallel fault planes. The faults are layer parallel and seen within the IPMS unit. Timing relationships between these faults and the Walter-Outalpa shear zone is unclear, however both transect the amphibolite dyke which intrudes the IPMS and WG lithologies. The faults strike at a high angle to the shear zone (105°). These faults are only 100 metres north of the main shearing, and only recognisable through the offset of the amphibolite. This horizontal offset is only 10m. One minor-scale fault is seen to transect an F_3 fold (Plate 3.c), therefore this

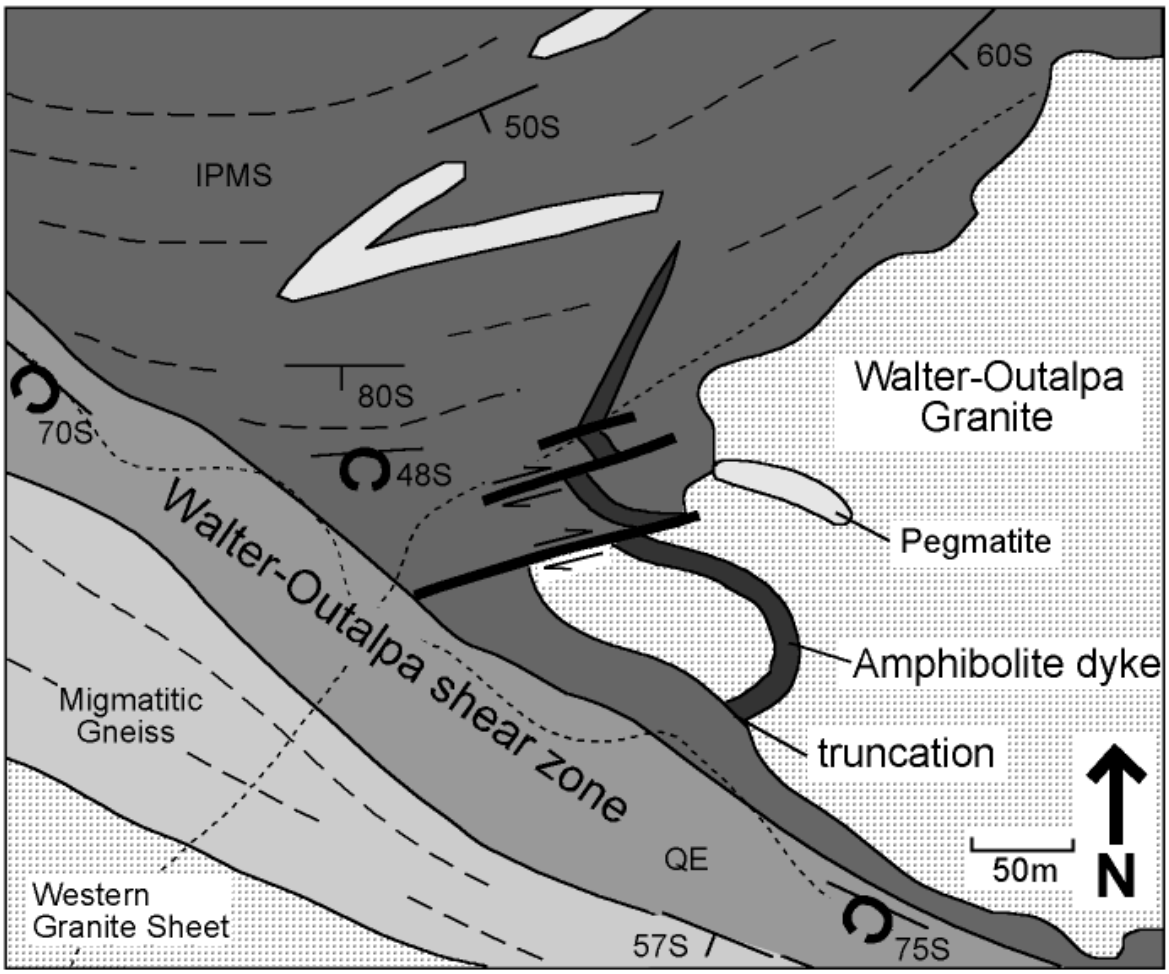

Figure 5.8 Apparent dextral fault offset of an amphibolite dyke which intrudes the IPMS and Walter-Outalpa Granite, but is sheared by the shear zone. Interaction between the NE trending faults and the Walter-Outalpa shear zone is not confined.

faulting is younger than the Olarian deformation, and probably Delamerian in age.

In two other creek beds (Figure 3.1), fault gouge material is found. These are discontinuous however, and only seen in the creek bed. Both are typically 1 metre thick, and contain highly recrystallised and fine-grained quartz aggregates. The matrix of the eastern fault gouge is prominently chlorite, muscovite, quartz, and plagioclase. Quartz aggregates are less angular within this example. The western fault gouge is highly angular and contains a carbonaceous matrix. Other lithologies within the creek bed do not contain carbonaceous material; therefore this may indicate a fault that was active during the Delamerian.

5.2.2 e) *Lineations*

Lineations relating to shear zone displacement are defined most clearly by mineral lineations and slickensides. Mineral lineations are represented by the elongate growth of chlorite and sericite within the schists. Quartz and micas form this lineation within the gneisses. Slickensides are represented most prominently on quartz (Plate 3.d) and pegmatite veins.

Lineations relating to shear zone displacement consistently plunge 41° towards the SE. The dextral sense of shear zone structures, and southerly dip of shear planes, along with 'step' analysis of slickensides and mineral growth, indicates an oblique reverse sense of movement of the shear zone. Shear zone lineations have an average plunge of 41° towards 126°. Shear zone lineations are formed by chlorite and muscovite which are Delamerian in age (See Chapter 5.4, Sm-Nd Dating of the Shear Zone).

Shear zone displacement has also caused the formation of related shear zone lineations. These however form on the conjugate riedel and anti-riedel planes. Mineral elongation lineations and slickensides preserve this movement. These lineations are only seen on the quartz-rich blocks, they are not seen in the protomylonitic ductile schists. Therefore most shear zone displacement lineations are measured in the ductile protomylonitic schists. No pre-Delamerian lineations are recognisable within the Walter-Outalpa shear zone.

5.2.3 Microstructures

The most useful microstructures within the Walter-Outalpa shear zone are found within the Garnet-chlorite Schist unit. Shear sense determination is possible with the presence of rotated porphyroblasts (Plate 3.e), pressure shadows (Plate 3.f), and S-C fabrics (Plate 3.g). Within this unit, structures are generally dextral, however there are some sinistral sense indicators.

The Retrograde Schist units also show the development of structures mentioned above. However these protomylonitic schists do not give reliable evidence of shear sense (Plate 3.h). There is not sufficient grainsize difference between porphyroblasts and groundmass (fabric minerals) to allow definitive rotation of porphyroblasts and therefore evidence of shear sense. Within most porphyroblasts of this unit, shear sense is indeterminable, or conflicting.

Elongate chlorite and muscovite compose the dominant shear fabric, and may even form an S-C fabric (Plate 3.g). Elongate aggregates of recrystallised polygonal quartz grains are also contained within this fabric. Magnetite is found both within the fabric, and

overgrowing it. This probably represents atleast two different ages of magnetite growth; fabric contained magnetite minerals are much finer. Little plagioclase is found within the shear zone, and none where there is ductile shearing. Plates 3.e-3.h display the array of microscopic structures and fabrics found within the shear zone.

5.2.4 Basement-Cover Interaction of Shear Zone

There is very clear evidence of shearing at the basement-cover contact. There is a conglomerate unit that defines Mawson's (1912) 'grand unconformity'. This is interpreted as the basal unit of the Adelaidean cover sediments and commonly has a thickness of approximately 2m. Where the shear zone interacts with the contact, this conglomerate can be seen to be up to 10m thick. This may indicate one of two things; either it represents sedimentary thickening, or it represents a stretching of the conglomerate to 5 times its original thickness by shearing.

Evidence for this stretching is preserved within quartz clasts of the conglomerate. These clasts show a mean object ellipse of 5.115, with $\phi = 0.20$ (Appendix 3), and an elongation direction parallel to the main displacement of the shear zone (ie. 41° towards 126°). A schistosity is also visible within this unit which is oriented parallel to the orientation of the Walter-Outalpa shear zone. Therefore it is evident that the shear zone was active after the basal conglomerate was deposited.

While this does indicate that the Walter-Outalpa shear zone was active during the Delamerian, there is strong evidence that the shear zone is much older than this, with a long active history. Horizontal displacements of the Walter-Outalpa Granite alone indicate up to 3500m offset. The basement-cover contact, while sheared, does not show discernible offset, especially of the order of that seen within the Willyama lithologies. Offset of this contact is obscured by alluvium.

Lithologies within the early Adelaidean Formations, particularly the Burra Group, tend to show localised folding of the order of tens of metres, which may be related to Delamerian reactivation of the shear zone. This reactivation is related to D_2 (Forbes, 1991). The fold axes lie parallel to the shear zone orientation, and these particular folds are only found in the Burra Group within proximity to the Walter-Outalpa shear zone. Andrews (1922), Binns and Miller (1963), and Glen *et al*. (1977), noted this relationship of retrograde shear zones causing localised cover folding within other regions of the OD.

5.2.5 Shear Zone Geometry

The geometry of the Walter-Outalpa shear zone may be constrained with confidence by detailed analysis of shear zone structures. The relationship of shear zone structures to strain, allows examination of strain conditions that prevailed during shearing. Structures represented within the Walter-Outalpa shear zone are from Delamerian reactivation as they are formed by Delamerian aged minerals.

The formation of a strain ellipse diagram is generated from the measurement of minor-scale structures within the shear zone (Figure 5.7). C planes within the shear zone indicate that the bulk shear plane strikes 112°, and dips 67°S. Lineations present on these surfaces plunge 41° towards 126°, indicating the orientation of Delamerian displacement. Combined with dextral movement indicators, an oblique S over N shear zone may be interpreted. Riedel shear planes strike 134° and dip 65°S, at a low angle to the shear plane. Conjugate anti-riedel planes dip 60°W with a strike of 042°, at a high angle to the shear plane. Axial planes of shear folding strike 070° and dip relatively steeply. Fold axes however, average a plunge of 30° towards 250°. These orientations imply dextral shearing of folds in a direction aligned to the trend of shear zone lineations (Figure 5.9).

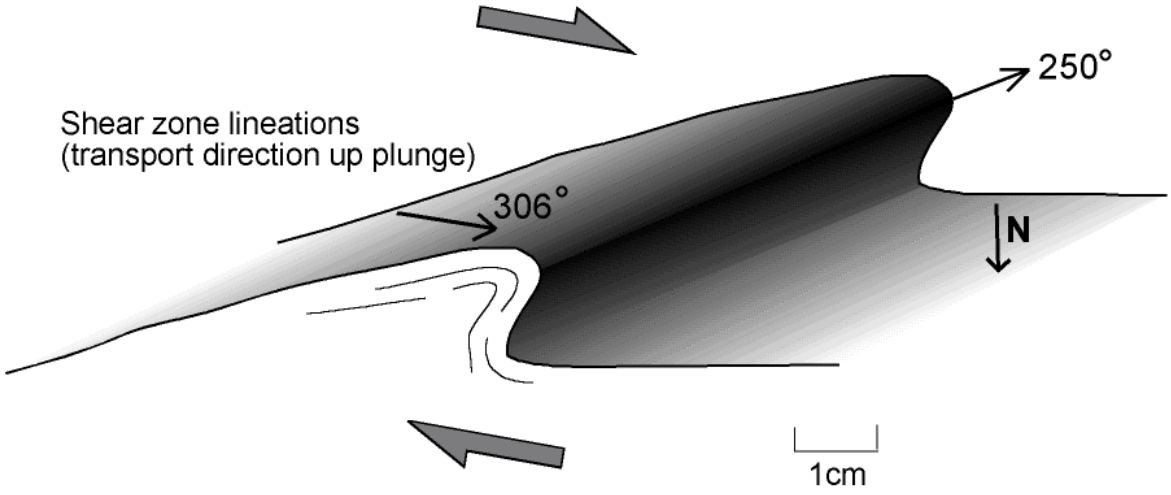

Figure 5.9 Sketch showing shear zone lineations (41° towards 126°) aligning with the transport direction (up plunge) of dextrally sheared asymmetrical folds.

The development of a strain ellipse diagram from these structures indicates approximately a N-S compression (σ_1) or shortening axis (Figure 5.7), as is also interpreted by Forbes (1991) for D_2. In this model, the σ_3 axis approximates an E-W elongation orientation. Similar strain axes are interpreted from a minor isoclinal fold sample (Figure 5.6) in which the fold axis is sheared by riedel shear planes, creating piercing points.

True displacements may be measured along riedel planes of this fold, offering minor-scale displacement across the shear zone. Four riedel shear planes show a cumulative displacement of 33.5mm over a distance of 50mm. If this represents a model for displacement, it might be expected that the Walter-Outalpa shear zone would displace lithologies 33.5m over a 50m wide shear zone. This model does not take three important factors into account however; 1) the effect of ductile shearing on displacement, 2) that the displacement shown has only occurred on riedel shear planes, and 3) *time*.

This model does not hold true when major-scale offset of the shear zone is measured. Offset measurement is possible between the WG and WGS. The amount of offset represented by these bodies is dependent on which limb of the WG the WGS sheared from. If the western limb of the WG relates to the WGS, horizontal offsets of 1,500m are seen. However, if the eastern limb relates, which has been interpreted from magnetic imagery (Conor pers comm., 1998), horizontal offsets up to 3,500m are indicated. This indicates that the shear zone has caused large displacements of lithologies relative to its width. Ductile shearing (including folding) may have played an important role in displacement of lithologies along the Walter-Outalpa shear zone. It is also interpreted that the shear zone has had a long history of activation, probably well before the Delamerian deformation, as *time* is the most important influence on displacement. A long period of time is required for a shear zone to displace 3,500m of rock, especially competent material such as granite.

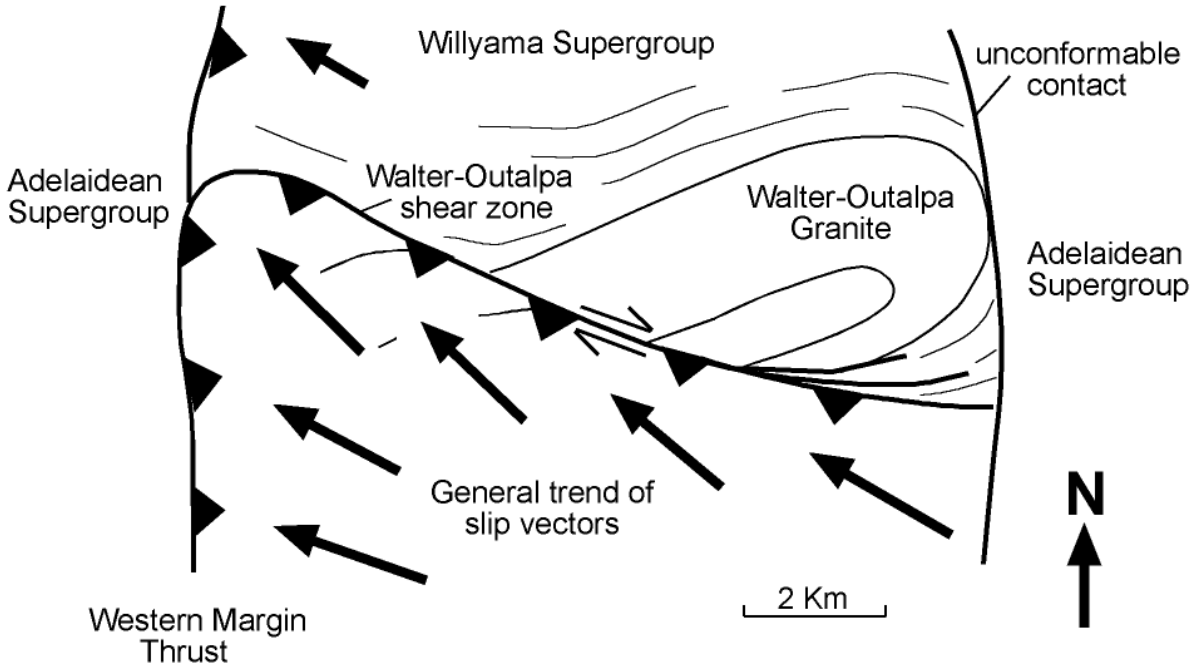

Figure 5.10 Schematic diagram for the general trend of slip vectors during western margin thrusting and reactivation of the Walter-Outalpa shear zone, within the eastern Weekeroo inlier. Based on field mapping and personal communication with Paul (1998).

The movement history of pre-Delamerian shearing is completely overprinted by Delamerian reactivation. Paul pers comm. (1998) has indicated through mapping that the shear zone fabric rotates into parallelism at its western extents with the N-S trending Delamerian (DD$_1$) shear zone. This represents a Delamerian overprint of the Walter-Outalpa shear zone, and both contain lineations which are oriented relatively parallel (Paul pers comm., 1998). This caused oblique shearing during the Delamerian, as seen in Figure 5.10 where the southern lithologies are thrust over their northern counter-parts.

5.3 Comparison with other Shear Zones

Little work has been documented on shear zones within the OD. Shear zones are extensive throughout the OD, and a variety of ages have been interpreted, based largely on timing relationships in the field. Two major timings of shear zone initiation have been determined, late stage OD$_3$ and DD$_1$. Late stage OD$_3$ retrograde shear zones, which are often referred to in text as retrograde 'schist' zones (Stevens, 1986), display ductile shearing (Ashley *et al*., 1998) with the formation of mylonitic 'fins' which often define ridges. These most often trend E-W and at locations such as Crockers Well, and Radium Hill, they have controlled the distribution of U and REE mineralisation (Flint and Parker, 1993). Extensive brittle phases of shearing, which are present within the Walter-Outalpa shear zone, are not present within the retrograde 'schist' zones. Brittle structures within the Walter-Outalpa shear zone are interpreted to have formed during Delamerian reactivation. This may indicate that the orientation of the Walter-Outalpa shear zone, NW as compared to E trending 'schist' zones, allowed more pervasive Delamerian reactivation of the Walter-Outalpa shear zone than that seen along the 'schist' zones. However, it may just be a result of the sheared lithologies within the Walter-Outalpa shear zone having a higher competency level than that of other shear zone lithologies. The retrograde 'schist' zones have been interpreted as late OD$_3$ structures based on field timing relationships, their retrograde mineral assemblages, and similar orientations of the shortening axis to that of OF$_3$ folds (Clarke *et al*., 1986). At the eastern margin of the Walter-Outalpa shear zone, a zone of shearing approximately 1500m in length and up to 40m wide significantly resembles documented retrograde 'schist' zones (Stevens, 1986).

Until this study, the largest recorded offset along Olarian retrograde shear zones was of the order of 'a couple of hundred metres' (Ashley *et al*., 1998), on the E-W trending shear zones at Ameroo Hill. The Walter-Outalpa shear zone however, displays a horizontal offset up to 3,500m. To date, OD shear zones have not been studied for movement sense or offset.

It therefore is not possible to analyse the structural relationships between the E-W trending 'schist' zones and the NW trending Walter-Outalpa shear zone.

Delamerian initiated shear zones are most prominently represented on the western margins of OD inliers. These are interpreted to have caused block rotation of the Willyama and Adelaidean Supergroups through E over W thrusting. The Walter-Outalpa shear zone rotates into parallelism with one of these Delamerian shear zones at the western margin of the eastern Weekeroo inlier.

5.4 Sm-Nd Dating of the Shear Zone

Isotopic analysis of a garnet-chlorite schist (Figure 3.1) within the shear zone was undertaken to give a recognisable date for the main shearing event. The presence of garnet allows the opportunity to use Sm-Nd geochronological techniques to date peak pressure and temperature in the shear zone, directly relating to the main phase of shearing.

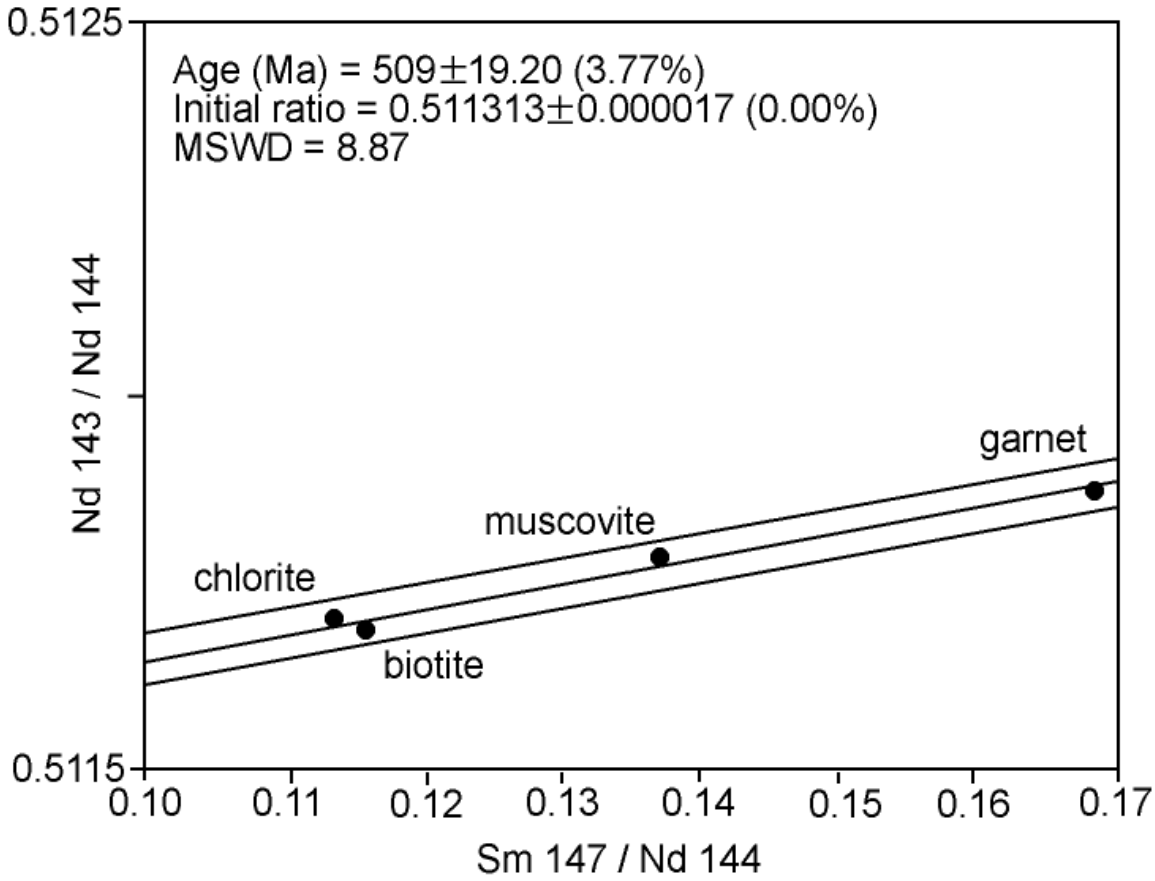

Figure 5.11 Garnet-chlorite-muscovite-biotite Sm/Nd isochron for the Garnet-chlorite Schist unit which is confined to the shear zone. Delamerian aged minerals indicate pervasive overprinting of the earliest shear zone minerals.

Samarium (Sm) and neodymium (Nd) are immobile REE and unlikely to be affected by alteration processes (McCulloch and Wasserburg, 1978). In the Sm-Nd system, radiogenic ^{143}Nd accumulates from its unstable parent ^{147}Sm. This is measured as a ratio from a reference non-radiogenic isotope, namely ^{144}Nd. This ratio is measured for mineral assemblages which grew in the same event and have remained as a closed system. Garnet, chlorite, muscovite, and biotite were separated and analysed to obtain Sm-Nd ratios. Ratios of $^{143}Nd/^{144}Nd$ and $^{147}Sm/^{144}Nd$ were plotted against one another and an isochron developed to best fit the plotted points. Garnet is a very useful mineral in Sm-Nd, because there is a large difference between their Sm and Nd partition coefficients (K_d). This therefore gives a point with a high $^{147}Sm/^{144}Nd$ ratio, which enables the development of an isochron with a reduced error.

Dating of the Walter-Outalpa shear zone using the Sm-Nd system (Figure 5.11) gives a Delamerian age for the main phase of shearing (509 ± 19Ma). It is not known whether the garnet minerals were reset by the Delamerian shearing or grew during this time. It is very likely that the latter is true. This date indicates that the earliest shear zone minerals and fabrics have been overprinted by the Delamerian shearing.

5.5 Discussion

Four models are interpreted for the evolution of the Walter-Outalpa shear zone. *Model 1* (Figure 5.12a) interprets a pre-Adelaidean, but post-OF_3 initiation of the shear zone. With the prominent Willyama offset occurring pre-Adelaidean, but small-scale structures and mineral assemblages representing Delamerian overprint (late DD_1 or DD_2, after thrust faulting and block rotation during DD_1). *Models 2*, *3*, and *4* (Figures 5.12b, 5.12c, and 5.12d respectively) interpret initiation of the Walter-Outalpa shear zone as being Delamerian as represented by the Delamerian age of the shear zone mineral assemblage. For this to be valid, the models imply that the 'grand unconformity' (Mawson, 1912) may be misinterpreted and the basal conglomerate represents a thrust zone (fault gouge) on the eastern margin of the eastern Weekeroo inlier. *Models 2* and *3* study the possibility of the thrusting on eastern and western margins of the inlier as being separate events, while *Model 4* studies the thrusts as being synchronous. The eastern Weekeroo inlier in *Model 4* would represent a 'pop up' structure on conjugate thrusts. In all models the major displacement of the Willyama Supergroup lithologies, occurred early in the shear zone history.

Figure 5.12 Models to interpret the evolution of the Walter-Outalpa shear zone. Model 1 is the preferred model as it accounts for all structures and relationships seen. Models 2 and 3 have a 180 degree change in the thrusting direction over a relatively short time period as well as many minor structural problems with the developed fabrics. Model 4 also has minor structural problems and can be easily tested in the field, with a detailed study of the unconformable contact.

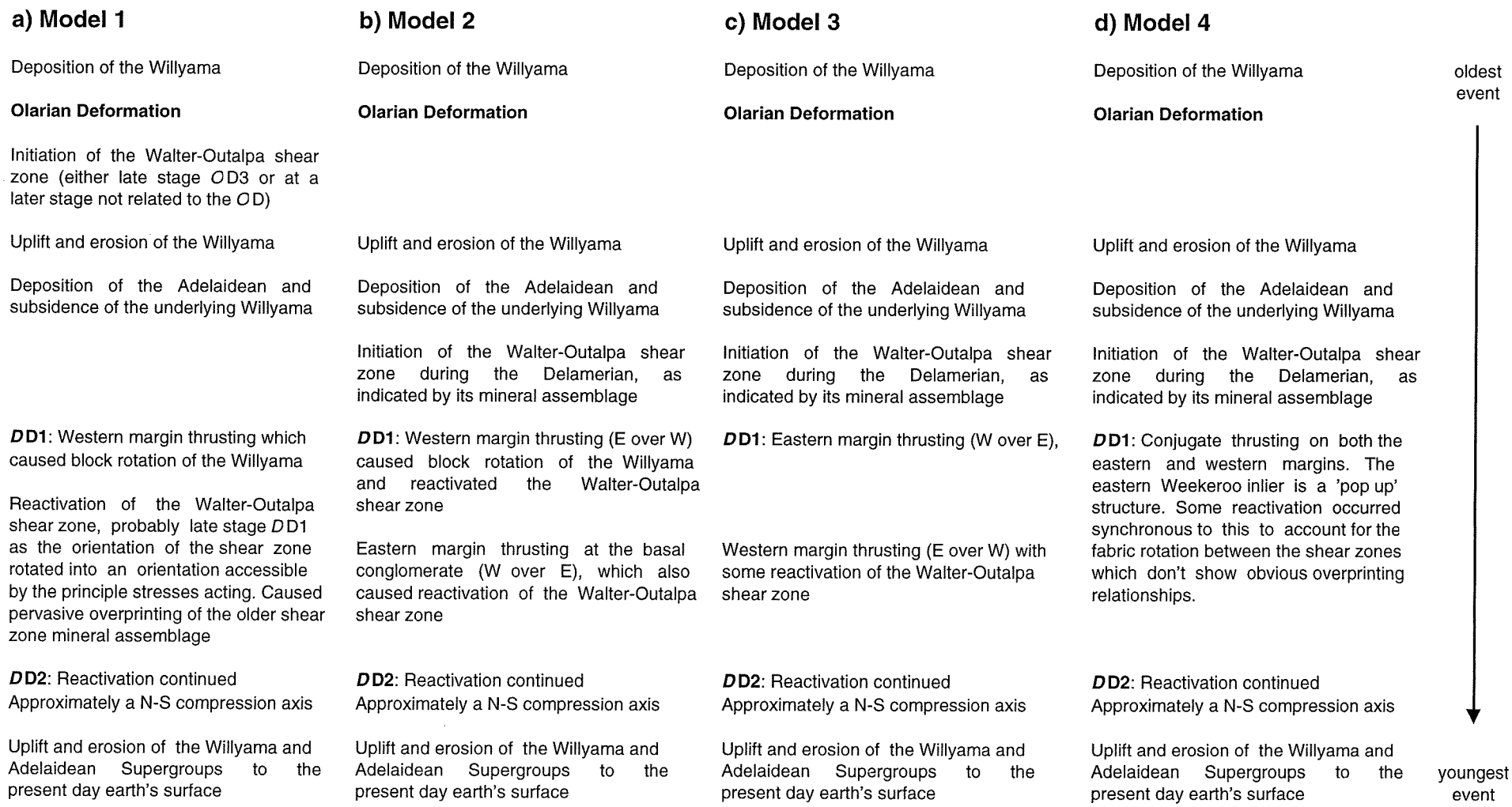

Model 1 (Figure 5.12a) is the preferred model, as it accounts for all structures and relationships within the shear zone, at the unconformable contact, and at the western margin thrust.

Model 2 (Figure 5.12b), with western boundary thrusting occurring before possible eastern boundary thrusting, would require two reactivation periods along the shear zone. The first to account for possible synchronous shearing with the western thrusting, in which the Walter-Outalpa shear fabric rotates into the western boundary shear zone and shows no overprinting criteria (Paul pers com., 1998). The second occurs to account for the shear fabric and clast elongation of the basal conglomerate aligned parallel to the orientation of the Walter-Outalpa shear zone.

Model 3 (Figure 5.12c) involves possible eastern boundary thrusting before western boundary thrusting. This model would only require one reactivation of the shear zone, in which shearing relationships on both boundaries of the inlier would be accounted for. *Model 3* is not able to allow for the presence of 'fault gouge' (brittle) lithologies within the early eastern boundary thrust, and ductile shear fabrics within the later western boundary thrusts.

Model 4 (Figure 5.12d) involves synchronous shearing of the western and possible eastern boundary thrusts. Shearing upon these two conjugate thrusts caused the Weekeroo inliers to act as large-scale 'pop up' structures (eg. Plate 2.h; small scale 'pop up' structures). Some reactivation along the Walter-Outalpa shear zone may have occurred as a late stage process of this to account for the fabric and clast elongation in the eastern boundary thrust being oriented parallel to the orientation of the Walter-Outalpa shear zone. The fabric within the eastern boundary thrust otherwise should be oriented parallel to the inlier boundary. This scenario does not account well for ductile fabric presence in the western boundary thrust, while the possible eastern boundary thrust shows a more brittle shearing phase, with the presence of a possible 'fault gouge' lithology.

Models 2, *3*, and *4*, may easily be tested with analysis of the basal conglomerate away from the shear zone interaction. The only small area of basal conglomerate that was studied away from shear interaction, was only studied briefly, and implied a typical unconformable contact unrelated to any thrusting contact. This indicates, along with minor structural problems in *Models 2*, *3*, and *4*, relating to their timing within the Delamerian deformation and folding, that *Model 1* describes the most probable evolution of the Walter-Outalpa shear zone.

Models 2, 3, and 4, do account well for the splaying nature of the shear zone, at the eastern end, towards the NE. This would represent rotation of the shear zone into parallelism with the possible eastern boundary thrust, as Paul pers comm. (1998) has indicated for the western boundary thrust and the Walter-Outalpa shear zone. Two models (Figure 5.13) to

MODEL 1

Trajectories of Maximum Instantaneous Stretch

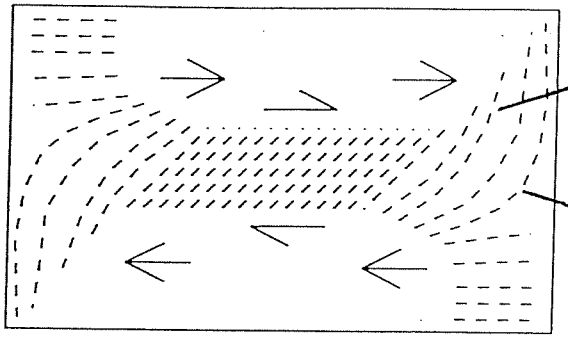

represents the splaying nature of shear bands at shear zone terminations

area of zero displacement - shear zone terminations are areas of zero displacement; WG shows an offset of 3,500m.

Shear Zone Terminations

(adapted from Hanmer and Passchier, 1991)

MODEL 2

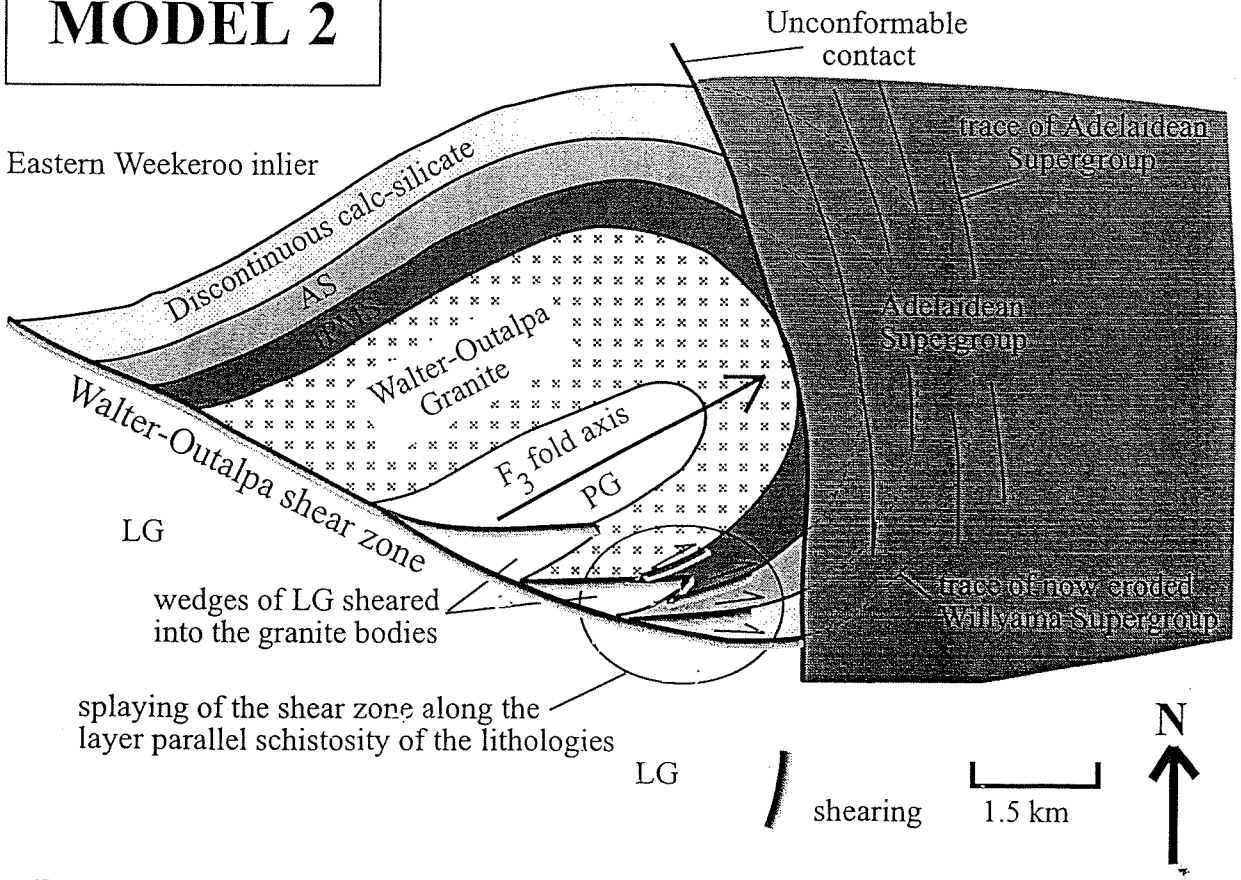

Figure 5.13 Two models to interpret splaying of the shear zone towards the NE, at the eastern end of the outcropping Walter-Outalpa shear zone. Model 1 - the eastern end represents shear bands splaying at a shear zone termination. Model 2 - the eastern end is an area where the schistosity of the lithologies folds around a major-scale F_3 fold into an orientation which allows shear bands to exploit.

relate this splaying to *Model 1* however have been developed, with the second model being preferred due to the amount of offset shown along the Walter-Outalpa shear zone.

CHAPTER 6 – Conclusions

The Walter-Outalpa shear zone is a NW trending feature which transects all lithologies and structures of the Willyama Complex. Adelaidean Supergroup lithologies close to the shear zone are folded, and the basal conglomerate, which marks Mawson's (1912) 'grand unconformity', contains a fabric and elongate quartz pebbles indicating it has been sheared.

Horizontal offset within the Willyama Supergroup is estimated up to 3,500m, however offset at the unconformable contact between the two Supergroups is insignificant. This indicates that the Walter-Outalpa shear zone initiated pre-Adelaidean, during which it was active for a relatively long period of time (to offset lithologies up to 3,500m).

Sm-Nd dating of the shear zone, using a garnet-chlorite schist, gives a Delamerian age (509 ± 19 Ma) for the mineralisation of garnet, chlorite, muscovite, and biotite. Garnet-chlorite schist is only present within the shear zone, and represents retrogressive shearing during Delamerian reactivation which overprints pre-Adelaidean shear zone mineral assemblages.

Shear zone structures are formed within these retrograde mineral assemblages, which indicates that they were also formed during Delamerian reactivation of the shear zone. The geometry of the shear zone, as indicated by these structures (Figure 5.7), only relates to the Delamerian processes acting on the shear zone.

During Delamerian reactivation of the shear zone dextral oblique-slip occurred, thrusting southerly lithologies northwestward. An approximately N-S shortening axis is estimated by the orientation of the strain ellipse, which is similar to that interpreted by Forbes (1991) during $D\mathrm{D}_2$.

Shear zone initiation is unclear, except to say that it occurred before the deposition of the Adelaidean Supergroup. It is clear that initiation was post-$O\mathrm{F}_3$ folding however, as the shear zone transects $O\mathrm{F}_3$ folds. Reactivation of the shear zone occurred either late stage $D\mathrm{D}_1$ or $D\mathrm{D}_2$, from block rotation (Paul pers comm, 1998) of the Willyama and Adelaidean Supergroups on N-S trending shear zones at the western margins of the inliers. All evidence along the shear zone consistently represents dextral shearing during the evolution of the Walter-Outalpa shear zone, with greenschist facies metamorphism during the Delamerian.

The pre-Adelaidean shear zone may have been completely ductile in nature, as is seen within E trending 'retrograde schist zones' (Stevens, 1986) of the Willyama Complex. However brittle-ductile conditions prevailed during Delamerian reactivation of the Walter-Outalpa shear zone.

Acknowledgments

There are many people who deserve acknowledgment for their help in the formation of this thesis. The help and support of Dr Pat James, my supervisor, is greatly appreciated. Thankyou for showing how to build on ideas, and weeding through nonsensical writing to help create a meaningful thesis. I thank Dr Kathy Stewart and Eike Paul for putting in much time and effort in helping with aspects of this thesis. Especially Dr Kathy Stewart, for her much needed guidance with geochronological techniques and interpretations. Thankyou Dr Thomas Flöttmann for assistance during the year, especially while in the field.

Special thanks must go to Colin Conor and the Department of Primary Industries and Resources of South Australia for their support both logistically and financially. This constant support of Honours projects provides great confidence to students and for that I am extremely grateful. Thankyou also to Trina Reif at PIRSA for organising the magnetic image for this thesis. Thankyou to Will and Pauline Crawford for allowing field work to be undertaken on the Weekeroo station during an important time of the year for them, it was appreciated very much.

The most funfilled thanks must go to my fellow *Weekeroo Boys* who made for a great time in the field, with many new life experiences (*What we do at Weekeroo must stay at Weekeroo*). Thanks Damian Brett, Martin Beck, Mike Szpunar (PIRSA), and especially 'Betsy' for everything (*Betsy can take you anywhere*).

The staff of the Geology Department have been enormously helpful over the whole year. I won't mention them all here because there are just *too* many people, but some important people were Gerald Buttfield, Wayne Mussared, Sherry Proferes, Sondra Gould, David Bruce, Ian Florance, and Kim Crawford. I appreciate your help more than you would ever realise.

I am very grateful for the strong support of my close family – Bryan, Jenny, Mark, Lee-anne, Mandy, Paul, Andrew, Eric, Anne, Kay, and of course Kyser and Sampson. Thankyou for your encouragement to achieve my goals. Thankyou also to Dr Potter and the Brighton Football Club for getting me healthy and providing a welcome release from study.

Finally, thanks must go to that crazy conundrum of characters that are the *1998 Honours Crew*. We've had some great times, and hopefully they will continue in the future.

If you're lost and feel on the road to nowhere,
Careful, Honours students are ahead.

References

AGSO, (1997) A transect of the Broken Hill inlier: notes for a workshop. *Broken Hill Exploration Initiative*. Australian Geological Survey Organisation. 47pp.

Andrews, EC, (1922) The geology of the Broken Hill district. *Mem. Geol. Surv. NSW.* **8**: 432pp.

Ashley, PM, Lawie, DC, Conor, CHH, Plimer, IR, (1997) Geology of the Olary Domain, Curnamona Province, South Australia, and field guide to 1997 excursion stops. Department of Mines and Energy South Australia. Report Book 97/**17**:51pp.

Ashley, PM, Conor, CHH, Skirrow, RG, (1998) Geology of the Olary Domain, Curnamona Province, South Australia. Field guidebook to Broken Hill Exploration Initiative excursion. Department of Primary Industries and Resources of South Australia. 53pp.

Behrmann, JH, (1987) A precautionary note on shear bands as kinematic indicators. *Journal of Structural Geology*. **9**:659-666.

Berry, RF, Flint, RB, Grady, AE, (1978) Deformation history of the Outalpa area and its application to the Olary Province, South Australia. *Trans. R. Soc. S. Aust.* **102**(2):43-53.

Berthé, P, Choukroune, P, Jegouzo, P, (1979) Orthogneiss, mylonite and non-coaxial deformation of granites: the examples of the South Armorican shear zone. *Journal of Structural Geology*. **1**: 31-24.

Biddle, KT, Christie-Blick, N, (1985) Glossary – Strike-Slip Deformation, Basin Formation, and Sedimentation. SEPM Special Publication. **37**:375-386.

Binns, RA, Miller, JA, (1963) Potassium-argon age determinations on some rocks from the Broken Hill district New South Wales. *Nature*. **199**: 274-275.

Blenkinsop, TG, Treloar, PJ, (1995) Geometry, classification and kinematics of *S-C* and *S-C* fabrics in the Mushandike area, Zimbabwe. *Journal of Structural Geology*. **17**(3):397-408.

Brett, DM, (1998) Structural, Geochemical and Isotopic Investigations of Granitoids within the Central Area of the Eastern Weekeroo Inlier, Olary Domain, South Australia. B. Sc. Honours thesis, The University of Adelaide.

Campana, B, King, D, (1958) Regional geology and mineral resources of the Olary Province. Geological Survey of South Australia. **34**:133pp.

Clarke, GL, Burg, JP, Wilson, CJL, (1986) Stratigraphic and structural constraints on the Proterozoic tectonic history of the Olary Block, South Australia. *Precambrian Research*. **34**:107-137.

Clarke, GL, Guiraud, M, Powell, R, Burg, JP, (1987) Metamorphism in the Olary Block, South Australia: compression with cooling in the Proterozoic fold belt. *Journal of Metamorphic Geology*. **5**:291-306.

Clarke, GL, Powell, R, Vernon, RH, (1995) Reaction relationships during retrograde metamorphism at Olary, South Australia. *Journal of Metamorphic Geology*. **13**:715-726.

Conor, C, (1998) Personal Communication. The Department of Primary Industries and Resources of South Australia.

Etheridge, MA, Cooper, JA, (1981) Rb/Sr Isotopic and Geochemical Evolution of a Recrystallized Shear (Mylonite) Zone at Broken Hill. *Contributions to Mineralogy and Petrology*. **78**:74-78.

Evernden, JF, Richards, JR, (1961) Potassium Argon Ages at Broken Hill, Australia. *Nature*. **192**:466.

Flint, RB, Parker, AJ, (1993) Willyama Inliers, in Drexel, JF, Preiss, WV, Parker, AJ (eds.) The Geology of South Australia. Volume 1. The Precambrian. Geological Survey of South Australia. Bulletin **54**:82-93.

Forbes, BG, (1991) Explanatory notes for the Olary 1:250 000 geological map. Geological Survey of South Australia. 47pp.

Forbes, BG, Pitt, GM, (1980) Geology of the Olary Region. South Australian Department of Mines and Energy, Report. BO/151.

Glen, RA, Laing, WP, Parker, AJ, Rutland, RWR, (1977) Tectonic relationships between the Proterozoic Gawler and Willyama Orogenic Domains, Australia. *Journal of the Geological Society of Australia.* **24**(3):125-150.

Hanmer, S, Passchier, C, (1991) Shear-sense indicators: a review. *Geological Survey of Canada.* **90**(17):72pp.

Hobbs, BE, (1966) The structural environment of the northern part of the Broken Hill orebody. *Journal of the Geological Society of Australia.* **13**:315-338.

Hobbs, BE, Vernon, RH, (1967) The structural and metamorphic history of the area around the northern half of the Broken Hill Lode. *Proc. Australas. Inst. Min. Metall. Proc. 8th Commonw. Min. Metall. Congr.* **6**:1419-1428.

Mawson, D, (1912) Geological investigations in the Broken Hill area. *Mem. R. Soc. S. Aust.* **11**: 211-319.

M^{c}Clay, KR, (1987) The Mapping of Geological Structures. John Wiley and Sons Ltd. England. 161pp.

M^{c}Culloch, MT, Wasserburg, GJ, (1978) Sm-Nd and Rb-Sr chronology of continental crust formation. *Science.* **200**:1003-1011.

Page, RW, Laing, WP, (1992) Metavolcanics related to the Broken Hill orebody, Australia: geology, depositional age and timing of high-grade metamorphism. *Economic Geology.* **87**: 2138-2168.

Paul, E, (1998) Personal Communication. The University of Adelaide, South Australia.

Ramsay, JG, Huber, MI, (1987) The techniques of modern structural geology, Volume 2: Folds and Fractures; Academic Press, London. 391pp.

Ramsay, JG, Graham, RH, (1970) Strain variation in shear belts. *Canadian Journal of Earth Sciences*. **7**: 786-813.

Ransom, DM, (1968) The relationship of lode shape to wall-rock structure in the southern half of the Broken Hill orebody. *Journal of the Geological Society of Australia*. **15**:57-64.

Richards, JR, Pidgeon, RT, (1963) Some age measurements on micas from Broken Hill, Australia. *Journal of the Geological Society of Australia*. **10**:243-260.

Stevens, BJP, (1986) Post-depostional history of the Willyama Supergroup in the Broken Hill Block, NSW. *Australian Journal of Earth Sciences*. **33**:73-98.

Talbot, JL, (1967) Subdivision and structure of the Precambrian (Willyama Complex and Adelaide System), Weekeroo, South Australia. *Transactions Royal Society of South Australia*. **91**:45-58.

Tchalenko, JS, (1970) Similarities Between Shear Zones of Different Magnitudes. *Geological Society of America Bulletin*. **81**:1625-1640.

Tourigny, G, Tremblay, A, (1997) Origin and incremental evolution of brittle/ductile shear zones in granitic rocks: natural examples from the southern Abitibi Belt, Canada. *Journal of Structural Geology*. **19**(1):15-27.

Vernon, RH, Ransom, DM, (1971) Retrograde schists of the amphibolite facies at Broken Hill, New South Wales. *Journal of the Geological Society of Australia*. **18**(3):267-277.

Williams, PF, (1967) Structural geology of the Little Broken Hill area, New South Wales. *Journal of the Geological Society of Australia*. **14**:317-331.

Willis, IL, Brown, RE, Stroud, WJ, Stevens, BJP, (1983) The early Proterozoic Willyama Supergroup: stratigraphic subdivision and interpretation of high to lowgrade metamorphic rocks in the Broken Hill Block, New South Wales. *Journal of the Geological Society of Australia*. **30**:195-224.

Appendices

1. Sm-Nd Isotope Geochronology
2. Figure and sample locations
3. Clast ellipticity analysis of basal conglomerate (Rf/ϕ plot)
4. Location of photographs for Plates 1-3

Appendix 1

Sm-Nd Isotope Geochronology

The sample was crushed in the jaw crusher and sieved to remove particles larger than 1mm. The remaining sample was then passed through the Wifley table to separate the sample into light, medium, and heavy fractions. The heavy mineral fractions were then passed through the Frantz magnetic separator. This yielded individual fractions which were enriched in the minerals of interest. From these separate samples, 200 Mg of garnet, chlorite, muscovite, and biotite were hand picked using a binocular microscope.

Dissolution of the samples was carried out in Teflon vials using HF-HNO3 and HF. Samples were then converted to chloride using 6N HCl. Samples were then split, with half of the sample being spiked with 150Nd-127Sm spike solution.

Sm and Nd samples were loaded on double degassed tantalum-rhenium filaments. Isotopic concentration (IC) measurements were carried out on a multicollector Finnigan MAT 262 Mass Spectrometer, collected in 10 blocks of 11 scans. Isotopic dilution (ID) measurements for elemental concentrations were carried out on a single collector Finnigan 261 Mass Spectrometer.

Measurements for Isochron Development

	biotite	muscovite	chlorite	garnet
Nd ppm	171.383	22.452	161.730	22.051
Sm ppm	32.834	5.082	30.333	6.135
143/144 Nd	0.511681	0.511782	0.511697	0.511870
2 sigma	0.000006	0.000007	0.000008	0.000008
Sm/Nd	0.1916	0.2264	0.1876	0.2782
147Sm/144Nd	0.1159	0.1369	0.1135	0.1683

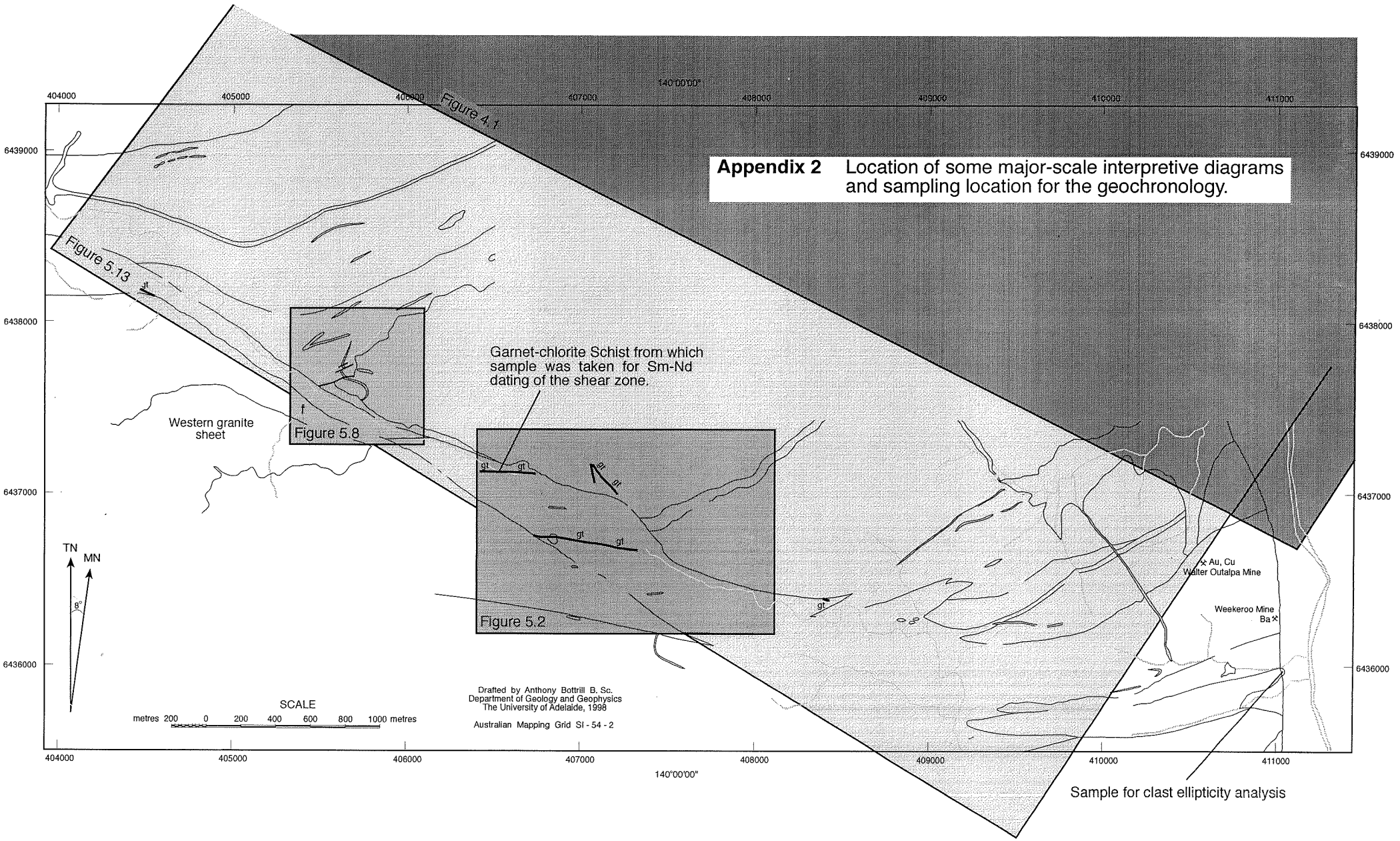

Appendix 2 Location of some major-scale interpretive diagrams and sampling location for the geochronology.

Appendix 3 Rf/ϕ Plot to show ellipticity of clasts within the basal conglomerate at the boundary between the Adelaidean and Willyama Supergroups.

INSTRAIN 2.5: INTEGRATED STRAIN ANALYSIS

Project: Appendix 3
Data File: tab1.a
Number of Objects: 54 defined by 4 points each.

Sample ID: Basal conglomerate
Surface Orientation:

Rf/Phi Plot: Mean Object Ellipse

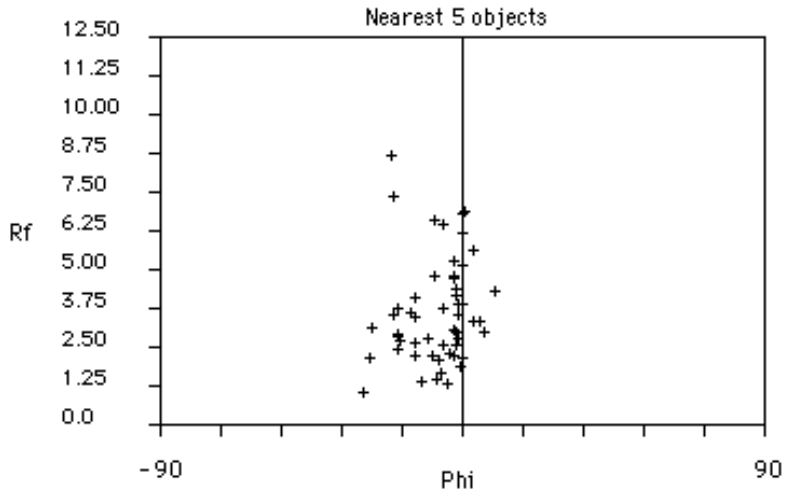

Ellipticity Range: 1.051 to 8.681

MEANS (+/- 1 STD)

Phi (degrees) : -7.650 +/- 9.206
X/Y (n = 53)
Arithmetic 3.637 +/- 1.702
Harmonic 2.938

Mean Object Ellipse: X/Y = 5.115 Phi = 0.20
Average error: -2147483648.-2147483648 %

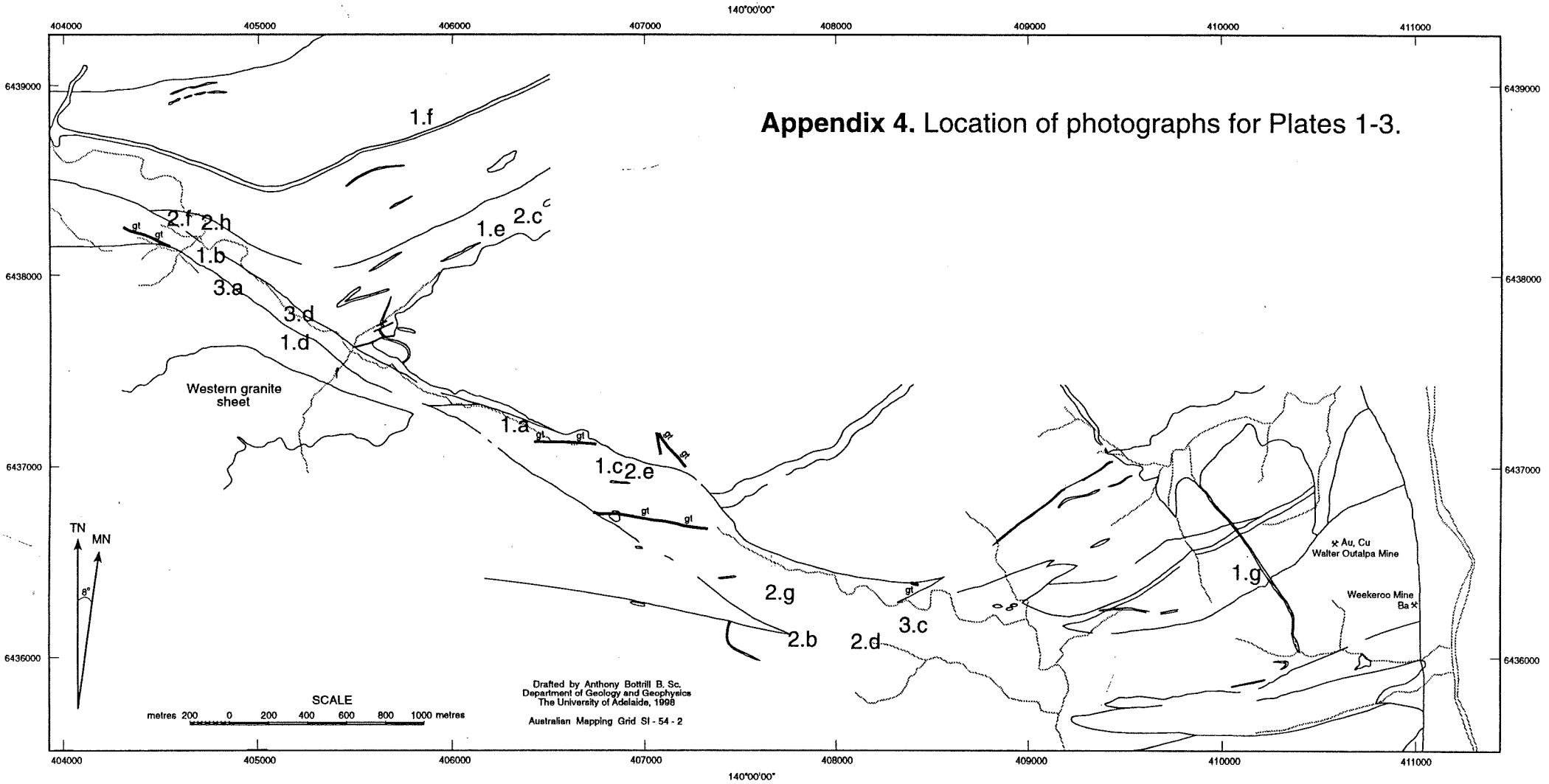

Appendix 4. Location of photographs for Plates 1-3.